

United States
Environmental Protection
Agency

Environmental Sciences Research
Laboratory
Research Triangle Park, NC 27711

EPA 600/3-83-024
April 1983

Research and Development

NTIS PB83-207407



Determination of Good-Engineering- Practice Stack Height

#11.50

A Fluid Model Demonstration Study for a Power Plant



RESEARCH REPORTING SERIES

Research reports of the Office of Research and Development, U S. Environmental Protection Agency, have been grouped into nine series. These nine broad categories were established to facilitate further development and application of environmental technology. Elimination of traditional grouping was consciously planned to foster technology transfer and a maximum interface in related fields. The nine series are

1. Environmental Health Effects Research
2. Environmental Protection Technology
3. Ecological Research
4. Environmental Monitoring
5. Socioeconomic Environmental Studies
6. Scientific and Technical Assessment Reports (STAR)
7. Interagency Energy-Environment Research and Development
8. "Special" Reports
9. Miscellaneous Reports

This report has been assigned to the ECOLOGICAL RESEARCH series. This series describes research on the effects of pollution on humans, plant and animal species, and materials. Problems are assessed for their long- and short-term influences. Investigations include formation, transport, and pathway studies to determine the fate of pollutants and their effects. This work provides the technical basis for setting standards to minimize undesirable changes in living organisms in the aquatic, terrestrial, and atmospheric environments.

DETERMINATION OF GOOD-ENGINEERING-PRACTICE STACK HEIGHT
A Fluid Model Demonstration Study for a Power Plant

by

Robert E. Lawson, Jr.

and

William H. Snyder

Meteorology and Assessment Division
Environmental Sciences Research Laboratory
U.S. Environmental Protection Agency
Research Triangle Park, NC 27711

ENVIRONMENTAL SCIENCES RESEARCH LABORATORY
OFFICE OF RESEARCH AND DEVELOPMENT
U.S. ENVIRONMENTAL PROTECTION AGENCY
RESEARCH TRIANGLE PARK, NC 27711

DISCLAIMER

This report has been reviewed by the Environmental Sciences Research Laboratory, U.S. Environmental Protection Agency, and approved for publication. Approval does not signify that the contents necessarily reflect the views and policies of the U.S. Environmental Protection Agency, nor does mention of trade names or commercial products constitute endorsement or recommendation for use.

The authors, Robert E. Lawson, Jr. and William H. Snyder, are physical scientists in the Meteorology and Assessment Division, Environmental Sciences Research Laboratory, U.S. Environmental Protection Agency, Research Triangle Park, NC. They are on assignment from the National Oceanic and Atmospheric Administration, U.S. Department of Commerce.

PREFACE

This report was prepared for the purpose of demonstrating the application of a fluid modeling approach to the determination of good-engineering-practice stack height. The approach follows the recommendations set forth in the Guideline for Use of Fluid Modeling to Determine Good Engineering Practice Stack Height (EPA, 1981).

ABS TRACT

A study using fluid modeling to determine good-engineering-practice (GEP) stack height for a power plant installation is discussed. Measurements are presented to describe the simulated boundary layer structure, plume-dispersion characteristics in the absence of the model plant building, and the maximum ground-level concentration of effluent downstream of the source, both with and without the model plant building. Analysis of the maximum ground-level concentrations shows that, in this case, a stack height of 64.1 m meets the current GEP criteria for 100% plant-load conditions.

CONTENTS

Abstract	iv
Figures	vii
Symbols	ix
Acknowledgements	xi
1. Introduction	1
2. Technical Approach	3
3. Examination Of Topography, Meteorological Parameters, And Selection Of The Area To Be Modeled	4
3.1 Topography	4
3.2 Meteorological parameters	4
3.3 Selection of modeled area	5
4. Evaluation And Justification Of Modeling Criteria	7
4.1 Similarity criteria	7
4.2 The model	9
5. Evaluation Of Simulated Boundary Layer	11
5.1 Boundary layer simulation	11
5.2 Dispersion comparability tests	13
6. Determination Of GEP Stack Height	16
6.1 Dispersion in the absence of the building	17
6.2 Dispersion in the presence of the building	21
6.3 Determination of GEP stack height	23
6.4 Plume rise	26
6.5 Discussion of results	27
7. Summary	31
References	32
Table 1	34
Appendices	
A. Description Of Facilities And Instrumentation	55
A.1 The Fluid Modeling Facility Wind Tunnel	55
A.2 Instrumentation	56
A.2.1 Velocity measurements	56
A.2.2 Concentration measurements	56
A.2.3 Data acquisition system	57
A.2.4 Volume flow measurements	58

CONTENTS (continued)

Appendices

B. Concentration Measurements For Stack Heights Of 54.2 m, 68.8 m, 72.3 m, And 90.3 m	61
C. GEP Stack Height For 50% Plant-Load Conditions	67
D. Raw Data Listings	70

FIGURES

<u>NUMBER</u>		<u>PAGE</u>
1	Topography, meteorological tower locations, and area modeled	35
2	Wind frequency distributions	36
3	Cumulative frequency distribution of wind speeds for northwest winds under neutral stability (valley tower location)	37
4	Vertical temperature profile in wind tunnel test section	38
5	Top and side views of the building	39
6	Schematic of the boundary-layer simulation system	40
7	Velocity profiles for the simulated atmospheric boundary layer	41
8	Turbulence intensity and Reynolds stress profiles	42
9	Lateral uniformity of mean velocity (a) and longitudinal turbulence intensity (b)	43
10	Surface concentration profiles (Δ) compared with Pasquill-Gifford C and D stability	44
11	Vertical concentration profiles compared with Pasquill- Gifford C stability	45
12	Lateral concentration profiles compared with Pasquill- Gifford C stability	46
13	Plume widths compared with Pasquill-Gifford curves	47
14	Flow visualization with and without the primary facility model (paraffin-oil smoke source). $H_s = 64.1$ m, 100% plant load	48
15	Vertical profiles of mean velocity and longitudinal turbulence intensity downstream of the model building	49

FIGURES (continued)

<u>NUMBER</u>		<u>PAGE</u>
16	Vertical profiles of vertical turbulence intensity (a) and Reynolds stress (b) downstream of the model building ...	50
17	Surface concentration profiles with (Δ) and without (\square) the building. Stack height 64.1 m	51
18	Vertical concentration profiles with (Δ) and without (\square) the building. Stack height 64.1 m	52
19	Vertical concentration profiles with (Δ) and without (\square) the building. Stack height 64.1 m, downstream distances of 1.5 km and 1.7 km respectively	53
20	Lateral concentration profiles with (Δ) and without (\square) the building. Stack height 64.1 m, downstream distances of 1.5 km and 1.7 km respectively	54

SYMBOLS

d	displacement height [L]
D	stack diameter [L]
H	structure or obstacle height [L]
H_B	building height [L]
H_g	GEP stack height [L]
H_s	stack height [L]
L	lesser dimension (height or width) of structure [L]
Q	tracer volumetric flow rate [L^3/T]
Re_B	building Reynolds number
Re_s	effluent Reynolds number
u'	streamwise fluctuating velocity [L]
u^*	friction velocity [L]
U	wind speed [L/T]
U_B	wind speed at top of building [L/T]
U_s	wind speed at stack height [L/T]
U_∞	free-stream wind speed [L/T]
W	stack effluent exit velocity [L/T]
W'	vertical fluctuating velocity [L/T]
x	streamwise coordinate [L]
y	cross-stream coordinate [L]

SYMBOLS (continued)

z	vertical coordinate [L]
z_0	roughness length [L]
δ	boundary layer depth [L]
ϵ	gravel size [L]
ν	kinematic viscosity [L^2/T]
ρ_s	effluent density [M/L^3]
ρ_a	density of ambient air [M/L^3]
σ_y	horizontal dispersion parameter [L]
σ_z	vertical dispersion parameter [L]
x	concentration [M/L^3]
x_{g1}	concentration at ground level [M/L^3]

ACKNOWLEDGMENTS

The assistance and cooperation of the following individuals are gratefully acknowledged: Mr. R.D. Jones for his painstaking efforts in collecting the data; Mr. Alan Huber for his many helpful discussions and comments; Ms. Carolyn Coleman and Ms. Eileen Ward for their patience in typing and assembling this report. Special thanks are due the Tennessee Valley Authority for providing the meteorological and plant operations data on which this demonstration study was based.

SECTION 1

INTRODUCTION

Section 123 of the Clean Air Act Amendments of 1977 defines Good-Engineering-Practice (GEP) stack height as "the height necessary to insure that emissions from the stack do not result in excessive concentrations of any air pollutant in the immediate vicinity of the source as a result of atmospheric downwash, eddies and wakes which may be created by the source itself, nearby structures or nearby terrain obstacles". The purpose of this study was to determine the GEP stack height for a power plant installation using fluid modeling techniques. The model was based on an existing facility, the TVA Widows Creek Plant, for which plant operating conditions, meteorological parameters, and detailed topographical maps were available. Almost every installation will have features that are unique; topographical and meteorological parameters are the most common of these features. Nevertheless, the fluid modeling approach is practical, and, if applied properly, should be useful in power plant design.

The general working rule for GEP stack height is:

$$H_g = H + 1.5L$$

where H_g is the GEP stack height, H is the height of the structure or nearby obstacle, and L is the lesser dimension (height or width) of the structure or nearby obstacle. Regulations to implement Section 123 of the 1977 Clean Air Act Amendments allow stack heights near structures as determined by the above equation to be used in establishing an emissions limitation plan.

Fluid modeling techniques may also be used to determine GEP stack heights

needed to prevent excessive pollutant concentration in the vicinity of the source. The maximum ground-level concentration measured in a model that includes nearby structures or terrain obstacles is termed "excessive" when it is 40% or more in excess of the maximum ground-level concentration measured in a model that does not include downwash, wake, or eddy effects produced by the nearby structures or terrain. The basic document that stipulates requirements for fluid modeling GEP studies is the Guideline for Use of Fluid Modeling to Determine Good Engineering Practice Stack Height (hereafter referred to as the "Guideline") (EPA, 1981). A more detailed reference, Guideline for Fluid Modeling of Atmospheric Diffusion (Snyder, 1981), provides technical standards for evaluation of various aspects of this study.

SECTION 2

TECHNICAL APPROACH

Bearing in mind that the height of the stack is creditable as GEP if the maximum ground-level concentration in the presence of the nearby building or obstacle is 40% greater than that measured in its absence, the ultimate objective of this study is to simply examine maximum ground-level concentrations as a function of stack height, in the presence and absence of a nearby structure or terrain obstacle. Other criteria specified in the Guideline must be met in order to validate the fluid-modeling approach. Certain steps specified in the Guideline must be followed when conducting any GEP fluid modeling study:

1. Examination of the topography and meteorological parameters, and selection of the area to be modeled.
2. Evaluation and justification of modeling criteria.
3. Evaluation of the test facility in the absence of buildings, other surface structures, or large roughness and/or elevated terrain.
4. Determination of the GEP stack height.
5. Documentation of the facility operation, instrumentation used in the study, and associated parameters.

These steps were followed and are reported in the following sections.

SECTION 3

EXAMINATION OF TOPOGRAPHY, METEOROLOGICAL PARAMETERS, AND SELECTION OF THE AREA TO BE MODELED

3.1 TOPOGRAPHY

The plant is in a river valley which extends southwest to northeast (figure 1); the river is southeast of the plant. A prominent ridge is located across the river, approximately 1.6 km southeast of the plant, and it parallels the river. This ridge rises rather abruptly (15° slope) to a plateau 250 m higher than the plant. To the northwest of the plant lies an area of gently rolling hills that extends approximately 7 km to an irregular plateau of about 300 m. The surface in this area is characterized by stands of pine trees and agricultural fields. The primary plant structure is a semi-rectangular building 36.3 m high, 159.5 m long, and 75 m wide. The longest dimension of the structure is parallel to the river (i.e., on a southwest-to-northeast line). Surrounding the building is generally flat terrain interrupted by several small auxiliary control buildings and an electrical distribution area. A second plant building is approximately 400 m northeast of the primary structure. The stack in question is between the primary structure and the river, 84.5 m southeast of the primary structure.

3.2 METEOROLOGICAL PARAMETERS

Meteorological data for one year were used to determine the air flow and stability characteristics in the plant vicinity. The locations of the meteorological monitoring towers are shown in Figure 1. The valley-site tower is about 1.2 km southwest of the plant; the mountain-site tower is approximately

4 km southeast of the plant, and is situated on the plateau. Wind speed, wind direction, and temperature data were recorded on the towers at heights of 10 m and 61 m. The data available from these towers consisted of joint frequency distributions of wind speed and direction, by stability class. The wind frequency distributions for all stability categories and for neutral stability for both valley and mountain locations are presented in Figure 2. The mountain site data reflected a reasonably uniform distribution for all stability classes; for neutral conditions, the predominant wind direction was from the northwest. The valley site data demonstrated the strong influence of the valley in channeling the air flow; the predominant wind for all stability classes was along the valley. In neutral stability, there was again a strong component along the valley, with a secondary maximum for northwest winds. Analysis of the climatological data by Hanna (1980) showed the roughness length characteristic of the upstream fetch to be approximately 1.0-1.5 m for the mountain site; the valley site exhibited values of 0.7-1.6 m for flow along the valley and 0.2-0.6 m for flow normal to the valley. Hanna also pointed out that these values are probably representative of the fetch out to a distance of about 600 m from the plant building, and are reasonable considering the type of surface features surrounding the tower sites.

3.3 SELECTION OF MODELED AREA

The area within 100 m of the primary plant building was modeled in detail. The terrain outside this 100-m radius was modeled with surface roughness elements to a distance of 3.5 km upstream and downstream, and 0.8 km either side of the primary plant building. This area is outlined on Figure 1. The study was conducted with northwest winds under conditions of neutral atmospheric stability.

The building effects and ridge effects represent two different areas of study. In the present study, only the building effects during high-wind-speed, neutral conditions were examined. This limits the demonstration to situations without the complication of downwind terrain. In addition, proper scaling of the ridge southeast of the plant would have lead to a very small building model. This would have introduced the complication of small building Reynolds number. To determine the effects of plume dispersion and possible impingement on downwind terrain, further research will be necessary.

The northwest wind direction was chosen because it is normal to the largest dimension of the building. Under this condition, the dimensions of the building wake are greatest, and, hence, the downwash effect due to the building is maximized (Snyder and Lawson, 1976). The free-stream wind speed was selected by plotting the cumulative frequency distribution of wind speed for northwest winds under neutral stability (Figure 3). According to the Guideline, the design wind speed should be less than the speed that is exceeded less than 2% of the time for the given wind direction. This 98th-percentile wind speed is 8.0 m/s for the 61-m valley tower site. This corresponds to a free-stream wind speed of 11.6 m/s (Section 4.2). The fetch which characterizes flow from the northwest is representative of gently rolling hills covered with stands of pine and agricultural fields. The surface roughness length is on the order of 0.2 to 0.6 m (Hanna, 1980). This appears consistent with the values of surface roughness length provided in the Guideline for surface types between palmetto and pine forest. Again referring to the Guideline, this range of surface roughness lengths corresponds to a u_{*}^2/U_{∞}^2 ratio from 0.0023 to 0.0026 and a power law index from 0.18 to 0.22.

SECTION 4

EVALUATION AND JUSTIFICATION OF MODELING CRITERIA

4.1 SIMILARITY CRITERIA

As specified in the Guideline there are five parameters in addition to geometric similarity that are relevant to modeling atmospheric flow. These are the Rossby number, Peclet number, Reynolds-Schmidt product, Froude number, and Reynolds number.

The Rossby number can be ignored here, because it represents the effects of the Coriolis force and is significant only when modeling effects greater than 5 km downstream from the source. The maximum downstream distance from the source that was modeled in the present study ranged from 3 to 4 km.

The Peclet number and Reynolds-Schmidt product are indicators of the importance of turbulent diffusivity, compared with molecular diffusivity (thermal and mass diffusivities, respectively). According to the Guideline, thermal and mass diffusivities are assumed to be negligible if the Reynolds number is high enough that advection and large scale turbulent motions are the primary mechanisms for dispersion.

The Froude number indicates the relative importance of inertial and buoyant forces. There are two Froude numbers that must be considered: the Froude number of the flow in the wind tunnel and stack Froude number. To model a neutrally stable (adiabatic) atmospheric flow in the wind tunnel, the Froude number of the flow in the test section must be infinite. This is equivalent to requiring isothermal flow in the tunnel. Figure 4

shows the vertical profile of temperature in the wind tunnel test section used in the study. The slight temperature gradient is of the order of -0.3°C in the lowest half-meter. This corresponds to a Froude number of approximately 57 which, for practical purposes, is neutral flow. The stack Froude number is an indicator of the buoyancy of the effluent in the ambient air. For precise scaling of buoyant releases, the Froude number of the model stack must match the Froude number of the prototype. The Guideline specifies that the ratios of stack diameter to building height, effluent density to ambient air density, and efflux speed to crosswind speed be matched between the model and prototype. The Guideline does not require that ratios of effluent buoyancy be matched. Hence, the stack Froude number was ignored.

The Reynolds number is the ratio of inertial to viscous forces acting on an air parcel. For a given fluid, strict matching of the model and prototype Reynolds numbers requires that the reference velocity be increased in direct proportion to the decrease in scale. As this is impractical for large reductions in scale, the principle of Reynolds-number independence is invoked to enable modeling under such conditions. Basically, the principle of Reynolds number independence states that the pattern of turbulent flow is similar at all sufficiently high Reynolds numbers. Two Reynolds numbers were considered in this study, the building Reynolds number (Re_B) and the effluent Reynolds number (Re_S).

$$Re_B = U_B H_B / \nu$$

where U_B is the wind speed at the top of the building, H_B is the building height, and ν is the kinematic viscosity of air. For sharp-edged buildings, the critical building Reynolds number, according to the Guideline, is 11,000. For the present model, which was sharp-edged, the building

Reynolds number was 13,400; hence, demonstration of Reynolds-number independence was not required.

The effluent Reynolds number is defined as:

$$Re_S = W_S D / \nu$$

where W_S is the efflux velocity, D is the stack diameter, and ν is the kinematic viscosity of the effluent. A sufficiently high effluent Reynolds number ensures that the effluent is turbulent; effluent from full-scale stacks is almost always turbulent. In the present study, the effluent Reynolds number of the model stack was approximately 8000 for full-load and 4000 for half-load plant operating conditions. The Guideline specifies that the effluent Reynolds number should preferably exceed 15,000, and that if it is below 2000, the flow should be tripped to induce turbulence. Since the effluent Reynolds number fell between these two values, the flow was tripped. A thin, internally serrated washer was inserted 10 stack-diameters upstream from the stack exit to ensure fully turbulent effluent flow.

4.2 THE MODEL

Values of parameters in the prototype and in the model are listed in Table 1. Figure 5 shows top and side views of the model building used in the study. The scale ratio selected, 1/430, was based on several considerations. Compromises were necessary to meet the opposing requirements of high Reynolds number and the limited length of the wind tunnel test section.

The other similarity criteria that were considered were the ratios of roughness length to boundary-layer depth, and building height to boundary-layer depth (Table 1). The model boundary layer had a depth of 0.9 m

and a roughness length of 0.74 mm and fit a power law profile with an index of 0.2 (Section 5.1). At a scale of 1/430, this provided a simulated roughness length of 0.32 m and a simulated boundary-layer depth of 387 m. The boundary-layer depth was somewhat lower than the Guideline recommendation, but it was consistent with examples shown by Davenport (1963). Also, because the ratio of the boundary-layer depth to the building height was large, the relatively thin boundary layer was not expected to significantly influence the results (Snyder, 1981). As no data were available on the full-scale boundary-layer depth, the roughness length was used as the primary means of comparing prototype and model. Measurements of turbulence spectra were not attempted; hence, no data were available for determining integral scales for either the prototype or model.

The model building and stack diameters were scaled to be geometrically similar to the prototype. Concentration measurements were initially made without roughening the model surface, because separated flow was expected to predominate near the sharp-edged model. In later tests, the model was covered with small gravel of size $\epsilon = 20 \nu / u_* (\sim 1.5 \text{ mm})$. No differences in measured concentrations were observed due to roughening the model. The effluent conditions to be modeled were based on full-load plant-operating conditions, and both the effluent density ratio and the effluent to wind speed ratio of the model were matched to the prototype. Table 1 also lists the stack effluent parameters. The values of the ratios of effluent to wind speed were in excess of 1.5, which means that they were high enough to preclude stack downwash.

SECTION 5

EVALUATION OF SIMULATED BOUNDARY LAYER

The arrangement evaluated in this section is the model flow in the absence of buildings, other surface structures, or large roughness and/or elevated terrain. The same arrangement, but with the plant building present, was used in the GEP stack height determination test.

5.1 BOUNDARY-LAYER SIMULATION

The method used for generating a simulated atmospheric boundary layer followed that of Counihan (1969) and is shown schematically in Figure 6. The arrangement consisted of a castellated barrier at the entrance of the test section, to trip the flow, followed by elliptical wedge vortex generators (which aid in shaping the velocity and turbulence intensity profiles), and surface roughness elements (which prescribe the surface layer characteristics and aid in maintaining the boundary layer once generated). Detailed geometry of the barrier, vortex generator, and roughness scheme used to generate the boundary layer for this study can be found in Castro and Snyder (1980). The surface roughness for the boundary layer consisted of discrete blocks, 27 mm X 27 mm X 18 mm high covering approximately 25% of the surface area. The advantage of the barrier, generator, and roughness scheme is that it produces a thick simulated boundary layer that develops very slowly after an initially rapid development.

As indicated in Section 4.1, the flow in the test section was essentially isothermal. The profile of Figure 4 is representative of condi-

tions during all tests. Since the entire test facility was enclosed in a temperature-controlled room, no significant temperature fluctuations occurred during the tests.

Figures 7-9 show the measured boundary-layer characteristics. Figure 7a shows the development of the velocity profile between 6 m and 15 m from the leading edge of the roughness. The development of the mean velocity profile is obviously quite rapid initially and quite slow thereafter, as there is little variation beyond 6 m. Using a displacement height of 18 mm, the mean velocity profiles all fit very nicely to a 0.2 power law. A semilogarithmic plot of the mean velocity profiles was used to determine the roughness length and surface shear stress (Figure 7b). All data are shown; however, only those points representative of approximately the lowest 250 mm (100 m in the prototype) of the simulated boundary layer were used to determine the best-fit log law. The roughness length was found to be 0.74 mm, and the square of the friction velocity, u_*^2 , was 0.045 (m/s)^2 . In Figure 8a, the longitudinal and vertical components of turbulence intensity are plotted as functions of height. The general shapes of the longitudinal turbulence intensity profiles are consistent with examples in the Guideline, but the absolute values of intensity are about 10% greater. The ratio of the vertical to the longitudinal component in the surface layer was approximately 0.5, and this is consistent with values typically found in the atmosphere. Figure 8b shows the shear stress normalized by the surface shear stress determined from the mean velocity profiles. Although there is considerable scatter, the data tend to collapse near the surface around a value of 1. The difference between this boundary layer and the naturally grown boundary layer

presented in the Guideline is that this one had a thicker constant stress region and greater shear stress in the early stages of development.

The model building was located 7 m downstream from the beginning of the roughness. This assured a reasonably well-developed boundary layer and a test section long enough to allow downstream measurements in the area of the maximum ground-level concentrations. Lateral profiles of mean velocity and longitudinal turbulence intensity (Figures 9a and 9b) were measured at several heights in the area between the model and the end of the study area (15 m). The greatest peak-to-peak variations occurred near the end of the study area and are attributed to effects of the tunnel exit section.

5.2 DISPERSION COMPARABILITY TEST

To establish dispersion characteristics of the simulated boundary layer, concentration profiles were measured in the downstream, lateral, and vertical directions through a neutrally buoyant plume. The source was a porous, sintered-bronze ball of 14 mm diameter. The ball was supported on the upstream side by a small-diameter tube, to minimize the influence of the support on the uniform tracer flow issuing from the ball. Ethylene gas was used as the tracer. The ball is effectively a point source. By using the ball instead of the standard stack, the problem of determining the effective stack height (i.e. physical stack height plus plume rise) was eliminated. Measurements were made with a model stack height of 233 mm, corresponding to a full-scale stack height of 100 m. The resulting measurements were converted to equivalent full scale concentrations in the form $\chi U_S / Q$ (m^{-2}), for comparison with dispersion estimates using Pasquill-Gifford stability categories C and D (Turner, 1970). The

vertical and lateral concentration profiles were used to calculate the mass balance of tracer at downwind positions.

Figures 10 - 13 present the data for the (100 m) stack. Figure 10 shows ground-level concentrations measured downstream with an estimate of the same using Pasquill-Gifford C and D stability classes. Pasquill-Gifford stability category C provides the best fit to the data for positions near and upstream of the maximum ground-level concentration. The comparison demonstrated that the boundary layer was slightly more turbulent than desired. Figures 11a and b show vertical profiles of concentration at four downstream locations (0.5 km, 1.0 km, 2.0 km, and 3.5 km) and predicted profiles, based on Pasquill-Gifford stability category C and a 100-m effective stack height. The use of 100 m as the effective stack height is supported by the vertical profile nearest the source. Here again, data from near the source fit the Pasquill-Gifford curves reasonably well. But, as the downstream distance increased, the values departed significantly from the curves. The rapid mixing of the plume into the surface layer is quite apparent. Lateral concentration distributions were measured at heights corresponding to the peak concentration found in the vertical profiles at 0.5 km, 1.0 km and 3.5 km from the source (Figure 12). Again the data have been compared with predicted concentrations using Pasquill-Gifford stability class C and 100-m effective stack height. The results are similar to those obtained for the vertical profiles; the Pasquill-Gifford predictions fit reasonably well near the source, but depart substantially farther downstream.

Using these vertical and lateral profiles together with the vertical

profiles of velocity, the quantity of tracer passing through each downwind cross section per unit time was calculated from

$$\iint [C(y,z) U(z)/Q] dy dz.$$

Ideally, this quantity should be near unity. Calculated values ranged from 0.99 nearest the source to 0.88 at the greatest downstream distance. Figure 13 shows the variation in vertical and lateral spread of the plume (σ_z and σ_y , respectively) with distance. The values of the lateral and vertical plume widths were derived from the concentration profiles by assuming Gaussian and reflected-Gaussian distributions, respectively. The solid lines represent Pasquill-Gifford stability categories C and D. The values of both σ_z and σ_y closely approximated those obtained with C stability, approaching D stability farther downstream.

In summary, the boundary layer dispersive characteristics were most closely approximated by Pasquill-Gifford stability class C (i.e., slightly unstable). The rate of decay beyond 1 km was slightly lower than that estimated from Pasquill-Gifford, resulting in some broadening of the concentration peak, but having little effect on the peak value. These results may be attributed, in part, to the larger roughness length and elevated source position of the model as compared to the smaller roughness lengths and ground-level sources most appropriate to estimates using the Pasquill-Gifford scheme. The growth rates of σ_z and σ_y with downstream distance were more consistent with those found by McElroy (1969) and Vogt (1977) in studies of dispersion over urban areas with roughness lengths on the order of 1 m.

SECTION 6

DETERMINATION OF GEP STACK HEIGHT

The determination of GEP stack height was based on the effect of the primary plant structure immediately upstream from the stack. The effect of the building was initially examined by flow visualization using a paraffin-oil smoke source. There was little observable difference in the plume characteristics except for very low stack heights where the plume was quite obviously directly entrained into the wake of the model building. Figure 14 shows two representative photos of the flow visualization tests with a stack height of 64.1 m and 100% plant load operating conditions. Plume rise estimated from these photos is approximately 45 m at 3.5 building heights downstream, and 65 m at 12 building heights downstream.

The model flow in the absence of the building was the same as that documented in Section 5; thus, no further measurements were needed to characterize the background flow. Flow characteristics in the presence of the model building are shown in Figures 15 and 16. Vertical profiles of mean velocity, longitudinal turbulence intensity, vertical turbulence intensity, and Reynolds stress were measured at three locations downstream of the model. Due to the response characteristics of the hot-wire anemometer, measurements taken in highly turbulent flows will reflect significant errors, and measurements taken in areas where flow reversal is frequent will reflect gross errors. Such measurements can be used only to compare areas of substantial flow distortion with and without the model building in place.

To find the GEP stack height, data were collected for four stack heights, 54.2 m, 68.8 m, 72.3 m, and 90.3 m. Excess concentrations of simulated pollutant were then analyzed and interpolated to find the stack height corresponding to the GEP criterion of 40% excess concentration. The GEP stack height was found to be 64.1 m. Documentation for this GEP stack height is included in sections 6.1 - 6.4; additional data used to determine the GEP stack height are included as Appendix B. Appropriate justification has been provided where deviations from the Guideline were deemed prudent.

6.1 DISPERSION IN THE ABSENCE OF THE BUILDING

The model stack was placed in the wind tunnel, and dispersion characteristics were measured in the absence of the model building. A model stack height of 149 mm was used, corresponding to a full-scale stack height of 64.1 m or 1.8 building heights. The stack effluent density ratio, ρ_s/ρ_a , and the effluent-to-wind-speed ratio, W_s/U_s , were matched between prototype and model. A mixture of helium, air, and ethylene was used to model the effluent; the ethylene served as the tracer, and the helium reduced the density of the model effluent mixture to 0.694. A two-minute sampling time with the free-stream wind speed of 4 m/s yielded reasonably stable average concentration values. Since the ethylene initially tended to cool the effluent significantly, a heat exchanger, consisting of a coil of copper tubing immersed in a container of water, was used to maintain the ethylene flow at nearly constant temperature. No heat exchanger was required for the air or helium flow. All concentration measurements were again converted to form $\chi U_s/Q$ (m^{-2}).

Longitudinal, vertical, and lateral concentration profiles were measured both with and without the model building, Figures 17 - 20. These plots were combined in order to facilitate direct comparison of the building's effects on downstream concentrations. Vertical concentration profiles were measured at three downstream distances: the location of maximum ground-level concentration, half-way between the source and the ground-level maximum, and approximately 3.5 building heights downstream of the source. Lateral concentration profiles were measured at the location of the ground-level maximum, both at the surface and at the elevation of the maximum concentration found from the corresponding vertical concentration profile.

Fewer vertical and lateral profiles were measured than specified by the Guideline. This is justifiable because the terrain is uniform; hence the plume is transported downstream with no significant lateral or vertical departure from the source location other than that due to plume rise or building effect. A model that included complex terrain features would certainly require a greater number of measurements to isolate adequately the location and value of the maximum concentration. The maximum ground-level concentration value in this study has been determined beyond a reasonable doubt.

The longitudinal ground-level concentration measurements without the building (Figure 17) showed that the peak concentration occurred approximately 1.7 km downstream of the source. Several measurements were taken near this location, not only to quantify the value of the peak concentration but also to determine the extreme (peak-to-peak scatter) concentration values. The peak value was $1.09 (\pm 0.08) \times 10^{-5} \text{ m}^{-2}$; thus, repeated measurements were within $\pm 7\%$ of the peak concentration. As shown in

Section 6.4, plume rise near the location of the ground-level maximum concentration was approximately 66 m, thus giving an effective stack height of approximately 130 m. Using this effective stack height, Pasquill-Gifford curves were constructed for stability classes C and D (Figure 17). When these curves are compared with the data, their results are very similar to those found in the dispersion comparability tests. C stability most closely approximates the experimental data, but again underestimates the peak concentration value. D stability grossly underestimates the peak concentration. This comparison again reflects the fundamental problem of comparing standardized dispersion parameters, which were based on ground-level sources and small roughness lengths, to situations characterized by elevated sources and relatively large roughness lengths. Since the comparison is very poor for D stability, only C-stability curves are shown in Figures 18 - 20 for comparison with the vertical and with the lateral concentration profiles.

Figure 19 shows the vertical concentration profile taken along the plume centerline at the location of maximum ground-level concentration. The data from nearest the surface are similar to the peak concentration value found from the longitudinal profile, while the concentration gradient in the vertical profile is seen to be very weak. This weak concentration gradient implies that errors in evaluating the peak ground-level concentration due to inaccuracies in sensor location were likely to have been quite small. Plume rise was on the order of 66 m. A more precise determination of plume rise was difficult due to the rather weak concentration gradient. Figure 18 shows the vertical concentration profile taken at downstream distances of (0.13 km) and (0.86 km). Plume rise

near the source was quite well defined, and was approximately 46 m at 0.13 km downstream and 61 m at 0.86 km downstream. Pasquill-Gifford curves for C stability are shown for comparison with the vertical profiles in the absence of the building. Once again these standardized curves offer a rather poor comparison to the experimental data.

Figure 20a shows the lateral concentration profiles taken at ground level through the location of peak concentration determined by the longitudinal profile. The value of the peak concentration was again consistent with the value taken from the longitudinal profile. The lateral gradient was somewhat weaker than that found in the vertical profiles. The peak concentration fell directly on the plume centerline; hence, beyond a reasonable doubt, the ground-level concentration peak has been located. Figure 20b shows similar profiles at the same downstream location but at an elevation corresponding to the maximum concentration found from the vertical concentration profile of Figure 19. Again, Pasquill-Gifford curves for C stability have been provided for comparison.

6.2 DISPERSION IN THE PRESENCE OF THE BUILDING

The model building was placed in the wind tunnel and concentration measurements were made for direct comparison with those made in the absence of the model building. Comparison of the two sets of data provided a direct assessment of the influence of the building's wake on downstream concentration. The stack height was again set at 149 mm (64.1 m full-scale); effluent conditions were identical to those used in the absence of the building (described in section 6.1). A two-minute averaging time was again found to yield reasonably stable average concentration values at the free-stream wind speed of 4 m/s.

A longitudinal profile of concentration downstream of the source was used to locate the maximum ground-level concentration. Subsequently, vertical and lateral concentration profiles were measured in order to establish beyond a reasonable doubt both the location and value of the ground-level maximum concentration. Vertical profiles were measured at three downstream locations: the location of the ground-level maximum, half-way between the source and the ground-level maximum location and approximately 3.5 building heights downstream of the source. Lateral concentration profiles were measured both at the surface and at the height corresponding to the elevated maximum concentration found from the corresponding vertical profile.

The longitudinal ground-level concentration measurements in the presence of the building (Figure 17) showed that the location of the peak concentration moved slightly closer to the source while the value of the peak concentration increased by approximately 40%. Several measurements

were again taken near the location of the maximum concentration, in order to determine the limits within which the concentration values fell. The maximum ground-level concentration was found to be $1.53 (\pm 0.11) \times 10^{-5} \text{ m}^{-2}$, with the peak-to-peak variation near the maximum on the order of $\pm 7\%$

Figure 19 shows the vertical concentration profile taken along the plume centerline at the location of maximum ground-level concentration. The data nearest the surface were in agreement with the peak concentration value found from the longitudinal ground-level profile. The concentration gradient near the surface was quite weak due to the increased turbulent mixing in the wake of the building. Plume rise, while difficult to estimate, was roughly 46 m, or 20 m less than that found in the absence of the building. Figure 18 shows the vertical concentration profiles taken at 0.13 km and 0.86 km. Plume rise near the source was again reasonably well defined and was approximately at 40 m at 0.13 km downstream and 56 m at 0.86 km downstream.

A lateral profile of concentration was taken through the ground-level maximum (Figure 20a). The peak concentration was again similar to that found from the longitudinal ground-level measurements, both in location (i.e. along the plume centerline) and in value. Several measurements were taken near the peak value in order to demonstrate that the random scatter in the measured values was of the same order of magnitude as that found from similar measurements near the peak of the longitudinal profile. Figure 20b shows the lateral profile taken through the plume centerline at the elevation corresponding to the peak of the vertical concentration profile. The measured concentrations were again consistent with those found from the vertical profile. In all cases, measurements

at the extreme lateral positions as well as the extreme vertical positions showed significant increases in random scatter due to the intermittent nature of the plumes near the edges. Peak values in all cases were at least two orders of magnitude greater than background; hence, the profiles were relatively smooth near the peaks.

6.3 DETERMINATION OF GEP STACK HEIGHT

The measurements described in sections 6.1 and 6.2 showed that, for a stack height of 149 mm (64.1 m full-scale), the maximum ground-level concentration in the absence of the building was located approximately 1.7 km downstream of the source and had a value of $1.09 (\pm 0.08) \times 10^{-5} \text{ m}^{-2}$. With the building in position, the maximum ground-level concentration was approximately 1.5 km downstream and had a value of $1.53 (\pm 0.11) \times 10^{-5} \text{ m}^{-2}$. The effect of the building was thus two-fold; the location of the maximum ground-level concentration moved approximately 13% closer to the source, and the value of the maximum ground-level concentration increased by 40%. A stack height of 64.1 m, or approximately 1.8 building heights, is then GEP in terms of excess concentration.

The plume rise measurements show that the effect of the building was primarily to lower the mean height of the plume. The additional turbulence created by the building wake tends to promote mixing of the lower portion of the plume, thus effectively transporting more tracer to the ground surface. The result of this mixing action was reflected in the weaker vertical concentration gradients and higher ground-level concentrations in the presence of the building. The lateral concentration

profiles of Figure 20 show that there was only a slight increase in the width of the concentration distribution at the surface.

When the general working rule for GEP stack heights

$$H_S = H + 1.5L$$

is applied to this case, the expected value for GEP stack height is 2.5 building heights or 90.3 m. With the fluid modeling approach, the value is 64.1 m (1.8 building heights), considerably lower than 90.3 m. Two factors contribute to the difference. The major factor is that the effluent-to-wind-speed ratio for the conditions modeled (100% plant load) was considerably greater than that on which the general working rule is based ($W_S/U_S = 3.5$ for the present case versus 1.5 for the general working rule). This additional momentum results in greater plume rise, hence decreasing the effectiveness with which the turbulent building wake can entrain the plume and thereby bring more tracer to the surface. Robins (1975), for example, showed that for a stack of 1.8 building heights above the center of a cubical building, the excess concentration was about 35% when the $W_S/U_\infty = 0.55$, but less than 20% when $W_S/U_\infty = 3.0$. In order to ascertain the effect of lowering the effluent-to-wind-speed ratio, measurements were made with 50% plant-load conditions (Appendix C). The fact that these results were in closer agreement with the general working rule substantiates the importance of the large effluent-to-wind-speed ratio.

The second important factor is the location of the source relative to the building. In the present case, the source was located approximately 2.5 building heights downstream of the building; the general working rule for GEP stack height is based on sources located immediately adjacent to or directly on top of the building. This separation between

the source and the building would certainly reduce the effect of the building wake on a plume emitted from the source. Huber et al. (1980) found that, for a model building with a height equal to one-half its length, the recirculating cavity region extended approximately three building heights downstream of the building. Using this figure as a guide, a source 2.5 building heights downstream may be outside the immediate influence of the most highly turbulent region of the building's wake. Barrett et al. (1978) found that the maximum ground-level concentration was reduced by approximately 15% when a stack of 1.8 building heights was moved from the center of a building to 2.5 building heights downwind. Their results, however, apply to cubical buildings oriented at 45° to the wind. Quantification of the effect of the separation of source and building is not possible in the present case without further experimentation. The implication is that the wake effect on the plume will be reduced when source and building are separated. The scatter in the maximum concentration values, while on the order of $\pm 7\%$ both with and without the building, resulted in a relatively large range of scatter in the excess concentrations. In fact, using the extremes of +7% error with the building and -7% without the building, a worst-case excess concentration of 60% (as opposed to 40%) was indicated. This corresponds to a possible worst-case GEP stack-height error of about ± 4 m. A more realistic and certainly more reasonable way to estimate the error in excess concentration is to assume that the errors in maximum concentration are normally distributed. The standard deviation is then on the order of one-sixth of the peak-to-peak value or about 2.3%. Using this standard error in the maximum concentration, the excess concentration is 47% (as

opposed to 40%), which corresponds to a GEP stack height error of about ± 1.5 m. This estimate of the error in measurement of excess concentration is based on a relatively small sample size and may be statistically questionable; however, it does provide some idea of the accuracy with which the excess concentration and, hence, GEP stack height can be determined.

6.4 PLUME RISE

The vertical concentration profiles without the building (Figures 18 and 19) were used to compare measured plume rise with calculated plume rise. Nearest the source ($x = 0.13$ km), the measured plume rise was 46 m. At downstream distances of 0.86 km and 1.7 km, the measured plume rise was 61 m and 66 m, respectively. Applying Briggs' (1975) plume rise formulation as specified in the Guideline, the predicted rise at these downstream distances was 49 m, 92 m, and 115 m. Agreement between predicted and observed plume rise is very good near the source (46 m v. 49). The discrepancies at the greater downstream distances are attributable to two factors: first, only the effluent density ratio and not the stack Froude number was modeled, thereby reducing the effects of buoyancy; and second, the large turbulence intensities measured in the simulated boundary layer lead to more rapid dispersion between the surface and the top of the stack. This had the effect of decreasing the distance over which turbulent entrainment occurs and as a result, the final rise was reached earlier than would be expected from a less turbulent boundary layer.

With the building model in place, plume rise near the source was reduced to approximately 40 m. Farther downstream, the differences in

plume rise with and without the building were difficult to quantify because of the weak vertical concentration gradients; however, the mean plume height did appear to be reduced. The data show that the mean plume height at 0.86 km downstream was approximately 120 m; therefore, the plume rise was about 56 m. At the location of the ground-level maximum, turbulence from the wake of the building had mixed the plume almost uniformly to the surface. Remnants of the elevated maximum can be seen at about 110 m, thus indicating plume rise of about 45 m. In the presence of the building, then, the plume initially rose much as it did in the absence of the building, however, shortly downwind it was more quickly mixed into the surface layer so that the mean plume height was lower.

6.5 DISCUSSION OF RESULTS

The effect of the building's presence was to move the location of maximum ground-level concentration closer to the source, thereby increasing the value of the maximum ground-level concentration and lowering the mean plume height. Since the effluent-to-wind-speed ratio was sufficiently large to preclude stack downwash, these effects must be attributable to the wake of the building. More precisely, it was the far wake which was primarily affecting the plume. Huber et al. (1980) pointed out that there are three distinct flow regimes found near a building in neutral flow. The undisturbed region, or free-stream, is the area outside the strongest influence of the building. Streamlines in this region may be slightly distorted as they pass over the building, but the turbulence levels remain essentially unchanged. On the lee side of the building, the flow is separated and a highly turbulent cavity region may exist. In this

cavity region, the flow near the surface is opposite the direction of mean flow. A plume which becomes trapped in this cavity is quickly mixed throughout the entire volume of the cavity by the highly chaotic flow. The extent of this cavity may vary from 2.5 to 10 building heights downstream, and depends upon the precise building shape and orientation. Downstream of the cavity region, a highly turbulent wake is found which decays with downstream distance. This far wake region is primarily responsible for the increase in maximum ground-level concentration in the present case. Even though the low-pressure cavity region may tend to limit initial plume rise somewhat, the effective stack height is sufficiently great to prevent the plume from being directly entrained into the cavity. This conclusion is supported by the longitudinal profiles of Figure 17. The additional turbulence downstream of the cavity, however, leads to more rapid diffusion of the plume, thus transporting it toward the surface. In the vertical concentration profiles at 0.86 km downstream and at the location of the maximum ground-level concentration, the vertical gradient of concentration was weakened considerably by the mixing action of the turbulence.

While the differences observed with and without the building have been shown to be related to the building wake effect, there are other factors that may result in adverse concentrations downstream of the source.

For the conditions examined in this report, the wind direction was perpendicular to the longest face of the building. This provided the greatest opportunity for wake effects by producing the largest wake. Though the frequency of occurrence is low, wind directions near 45° from

perpendicular may lead to trailing vortices, created by the building. Castro and Robins (1977) and Robins and Castro (1977) have shown, by indirect means, that a swirling wake consisting of two longitudinal, rotating vortices can produce downwash on the centerline. A plume within this wake could be drawn toward the surface, increasing ground-level concentrations substantially (Thompson and Lombardi, 1977). There is little available information with regard to the effect of building asymmetry or meandering of wind direction on these vortices; their strength and duration are difficult to estimate. Our cursory flow visualization exercises, however, did not reveal any effects of building asymmetry or meandering wind direction on plume behavior.

A second consideration with regard to wind direction is that winds from the east or southeast may downwash in the lee of the ridge that is 1.6 km southeast of the plant. Such downwash could again force the plume closer to the surface and create adversely high ground-level concentrations. Indeed, Lott (1982) reported that the highest surface concentrations measured during a field study at this site were caused by terrain-induced downwash resulting from neutral, southeasterly winds. As pointed out in section 3.3, a separate series of tests using a different model scale would be required to further evaluate the effects of this ridge.

The effects of stability are not so important with respect to the area immediately adjacent to the building. However, during very stable periods a plume from the stack may be transported with little vertical or horizontal dispersion, and may impact on the surrounding terrain. The most likely area for impact is again the ridge southeast of the plant; the conditions most likely to result in the highest surface concentrations

are where the plume elevation is just above a "blocked" layer (Baines, 1979), such that the plume grazes the surface of the slope as it is transported to the top. An evaluation of these effects, however, would require additional laboratory work and considerably more extensive meteorological data.

The effects of plant load were discussed in Section 6.3, and it should be emphasized that plant load is a very important factor in the determination of the GEP stack height. At very low plant loads, plume rise may be minimal and stack downwash may occur. When the plant load is very high, and winds are light the additional plume rise may mean that the plume is transported well downstream before encountering the envelope of the building wake. In this case the building influence will be minimized. For most installations, the average plant load will fall somewhere between these two extremes and may show considerable diurnal and seasonal variation. Where data are available, a correlation of plant operating conditions with wind direction and stability may be useful in justifying more appropriate plant load conditions. In the present demonstration study, only 100% plant-load operating conditions were considered in detail. Appendix C shows that a GEP stack height of 90.3 m (2.5 building heights) could be justified as GEP on the basis of 50% plant-load.

SECTION 7

SUMMARY

A fluid model study was conducted in a wind tunnel to determine the Good Engineering Practice (GEP) stack height for a power plant installation operating under 100% plant-load conditions. A stack height of 64.1 m was shown to meet the current GEP criteria.

The meteorological conditions simulated were northwest winds (the direction perpendicular to the face of the building) and neutral stability. Surface characteristics were modeled using surface roughness elements to simulate the terrain approximately 3.5 km upwind and downwind of the model building. The ratios of effluent density to ambient density and effluent speed to wind speed were matched between model and prototype, and the building Reynolds number was sufficiently high to ensure that the flow around the building was Reynolds-number independent. The background dispersion characteristics in the absence of the model were shown to conform most closely to Pasquill-Gifford stability category C, slightly unstable. Plume rise near the source was adequately described by Briggs' formulation. The effect of the building wake has been shown to decrease plume rise, decrease the downstream distance to the point of maximum ground-level, and increase the magnitude of the maximum ground-level concentration by 40%. Vertical and lateral concentration profiles both with and without the model building have been provided in order to show that the maximum ground-level concentration in each case has been determined beyond a reasonable doubt. The error in the measurement of excess concentration was on the order of $\pm 7\%$. The observed differences in maximum ground-level concentration with and without the building were shown to have resulted from the influence of the building wake.

REFERENCES

- Baines, P.G., 1979. Observations of stratified flow past three-dimensional barriers. J. Geophys. Res. 84 (C12): p. 7834-7838.
- Barrett, C.F., Hall, D.J. and Simmonds, A.C., 1978. Dispersion from Chimneys downwind of cubical buildings - A wind-tunnel study, Warren Spring Lab. presented at the NATO/CCMS 9th International Meeting on APMA, Toronto, Aug. 28-31.
- Bearman, P.W., 1971. Corrections for the effects of ambient temperature drift on hot-wire measurements in incompressible flow, DISA Information, no. 11: 25-30.
- Briggs, G.A., 1969. Plume Rise, Critical Review Series, U.S. Atomic Energy Commission. TID-25075. National Technical Information Service, Springfield, VA, 81pp.
- Briggs, G.A., 1975. Plume Rise Predictions. ATDL No. 75/15, Atmospheric Turbulence and Diffusion Laboratory, NOAA Environmental Research Laboratory, Oak Ridge, TN, 53pp.
- Castro, I.P. and Robins, A.G., 1977. The flow around a surface-mounted cube in uniform and turbulent streams. J. Fluid Mech. 79 (pt. 2): 307-335.
- Castro, I.P. and Snyder, W.H., 1980. Three Naturally Grown and Simulated Boundary Layers. Fluid Modeling Facility Internal Report, U.S. Environmental Protection Agency, Research Triangle Park, NC, July, 200pp.
- Counihan, J., 1969. An improved method of simulating an atmospheric boundary layer in a wind tunnel. Atmos. Envir. 3: 197-214.
- Davenport, A.G., 1965. The relationship of wind structure to wind loading. In: Proceedings of the Conference on Wind Effects on Buildings and structures, National Physics Laboratory, HMSO, London, pp. 54-102.
- Environmental Protection Agency, 1981. Guideline for Use of Fluid Modeling to Determine Good Engineering Practice Stack Height. EPA-450/4-81-003. U.S. Environmental Protection Agency, Research Triangle Park, NC. 47pp.
- Hanna, S.R., 1980. Measured sigma-y and sigma-theta in complex terrain near the TVA Widows Creek, Alabama, Steam Plant. Atmos. Envir. 14 (4): 401-407.
- Huber, A.H., Snyder, W.H. Thompson, R.S. and Lawson, R.E. Jr., 1980. The Effects of a Squat Building on Short Stack Effluents. EPA-600/4-80-055. U.S. Environmental Protection Agency, Research Triangle Park, NC, 118pp.

Khurshudyan, L.H., Snyder, W.H. and Nekrasov, I.V., 1981. Flow and Dispersion of Pollutants over Two-Dimensional Hills: Summary Report on Joint Soviet-American Study. EPA-600/4-81-067. U.S. Environmental Protection Agency, Research Triangle Park, NC., 143pp.

Lott, R.A., 1982: Terrain-induced downwash effects on ground level SO₂ concentrations. Atmos. Envir. 16 (4): 635-642.

McElroy, J.L., 1969. A comparative study of urban and rural dispersion. J. Appl. Meteorol. 8 (1): 19-31.

Robins, A.G., 1975. Plume Dispersion in the Vicinity of a Surface Mounted Cube, Central Electricity Generating Board, Research Department Report. R/M/R 220. Marchwood Engineering Laboratories, April.

Robins, A.G. and Castro, I.P., 1977. A wind tunnel investigation of plume dispersion in the vicinity of a surface mounted cube, I. The flow field. Atmos. Envir. 11 (4): 291-297.

Snyder, W.H., 1979a. Testimony on Behalf of the U.S. Environmental Protection Agency, Presented at the Public Hearing on Proposed Regulatory Revisions to the 1977 Clean Air Act Stack Height Regulations, Wash., DC, May 31, 12p.

Snyder, W.H., 1979b. The EPA Meteorological Wind Tunnel: Its Design, Construction, and Operating Characteristics. EPA-600/4-79-051. U.S. Environmental Protection Agency, Research Triangle Park, NC, 78pp.

Snyder, W.H., 1981. Guideline for Fluid Modeling of Atmospheric Diffusion. EPA-600/8-81-009. U.S. Environmental Protection Agency, Research Triangle Park, NC, 200pp.

Snyder, W.H. and Lawson, R.E. Jr., 1976. Determination of a necessary height for a stack close to a building - a wind tunnel study. Atmos. Envir. 10 (9): p. 683-691.

Thompson, R.S. and Lombardi, D.J., 1977. Dispersion of Roof-Top Emissions from Isolated Building: A Wind Tunnel Study. EPA-600/4-77-006. U.S. Environmental Protection Agency, Research Triangle Park, NC, 44pp.

Turner, D.B., 1970. Workbook of Atmospheric Dispersion Estimates. Office of Air Programs, Publication Number AP-26, U.S. Environmental Protection Agency, Research Triangle Park, NC.

Vogt, K.J., 1977. Empirical investigations of the diffusion of waste air plumes in the atmosphere. Nuclear Technol. 34: 43-57.

TABLE 1. PROTOTYPE AND MODEL PARAMETERS

Parameter	Prototype	Model
Scale	1	1/430
Free-Stream Wind Speed, U_{∞} (m/s)	11.6	4.0
Boundary Layer Depth, δ (m)	400(calculated)	0.9
Roughness Length, z_0 (m)	0.2-0.6	0.00074
u_*^2/U_{∞}^2	0.0023-0.0026	0.0028
Power Law Index	0.18-0.22	0.2
z_0/δ	0.00050-0.00150	0.00082
z_0/H	0.0056-0.0167	0.0088
Stack Diameter, D (m)	8.2	0.01905
Plant Load (%)	100	100
Effluent Velocity, W_s (m/s)	28.1	9.5
Effluent Temperature ($^{\circ}$ K)	422	293
Ambient Temperature ($^{\circ}$ K)	293	293
Density Ratio (ρ_s/ρ_a)	0.694	0.694
Effluent-to-Wind-Speed Ratio		
at Stack Exit ($H_s = 64.1$ m)	3.47	3.47

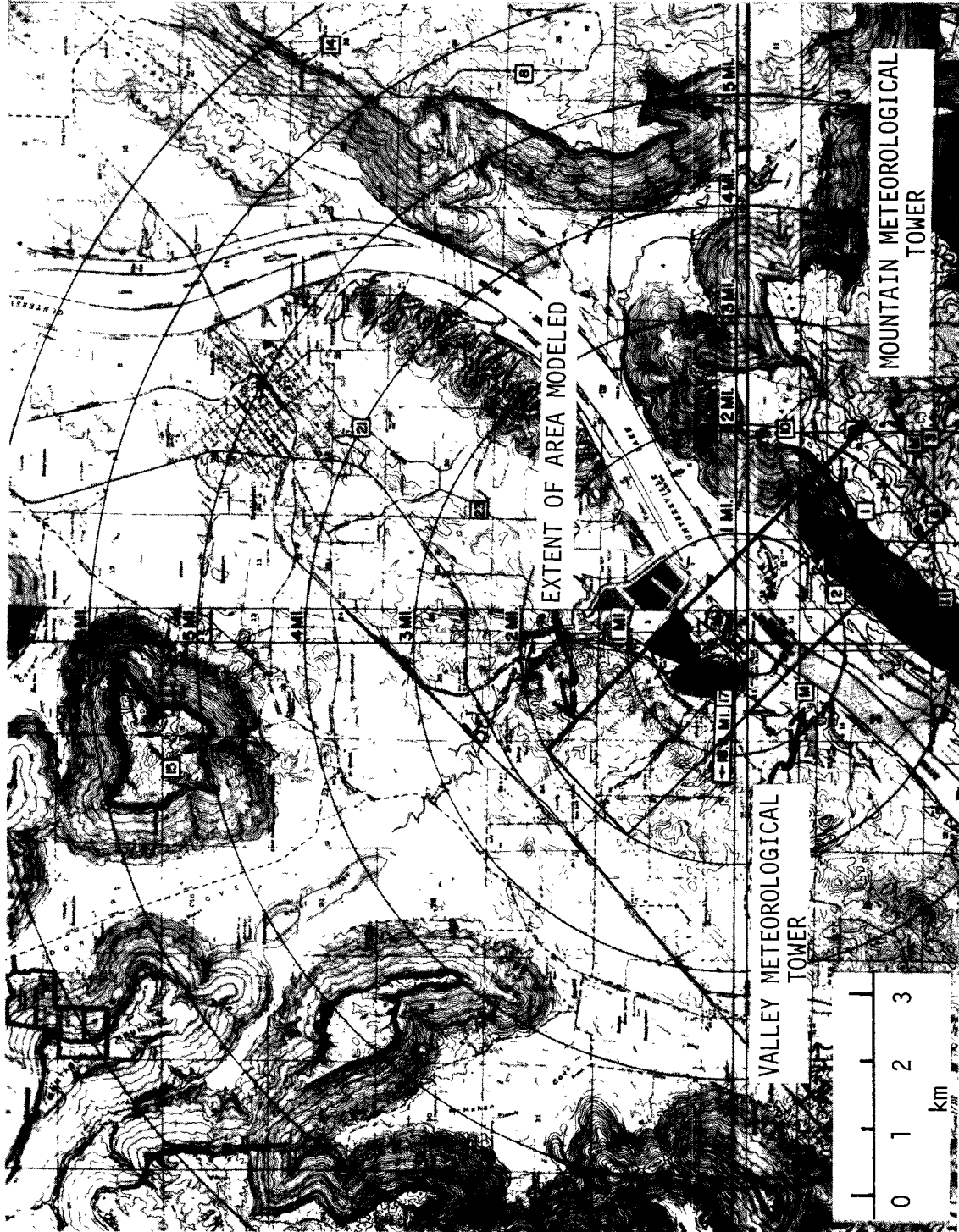


Figure 1. Topography, meteorological tower locations, and area modeled.

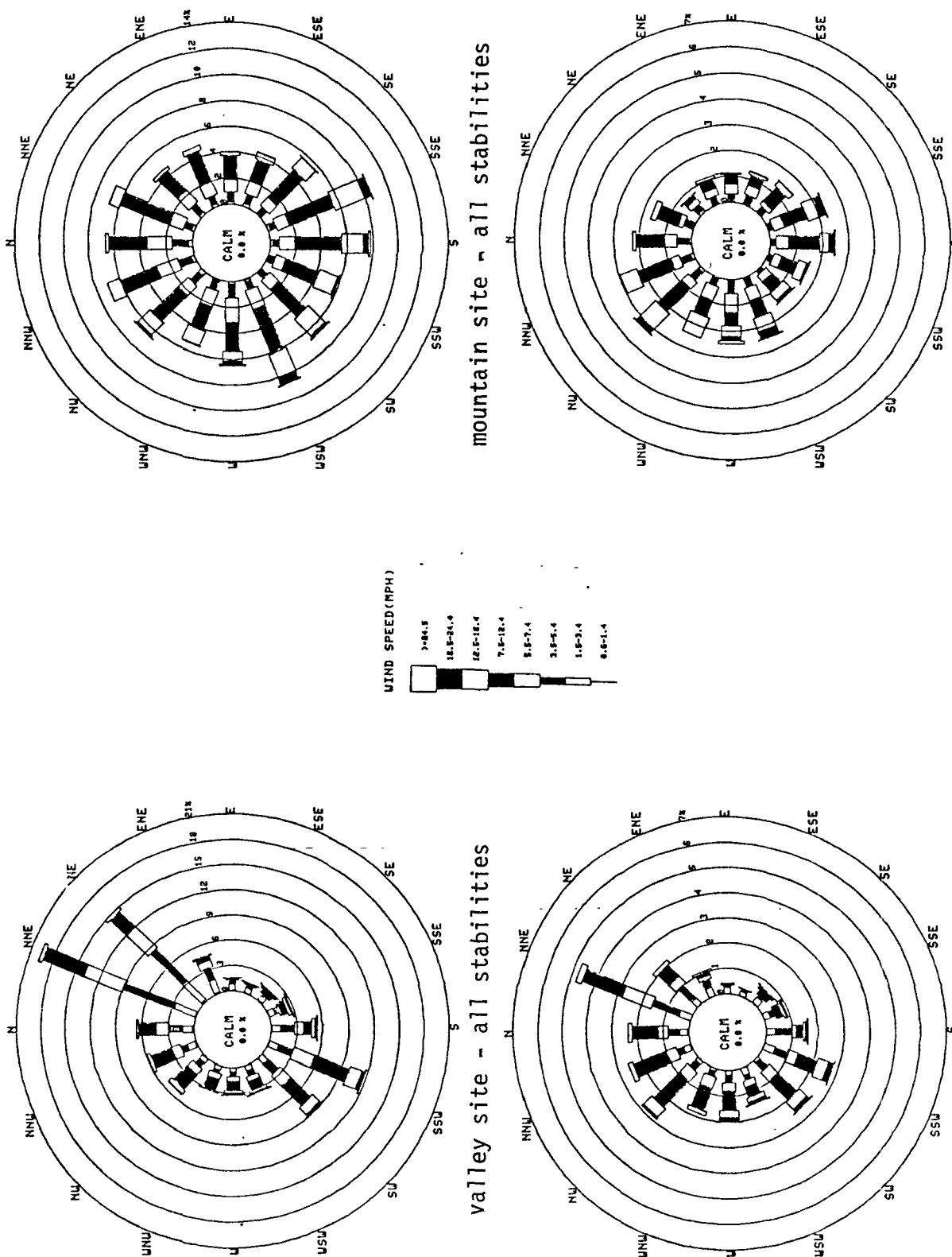


Figure 2. Wind frequency distributions.

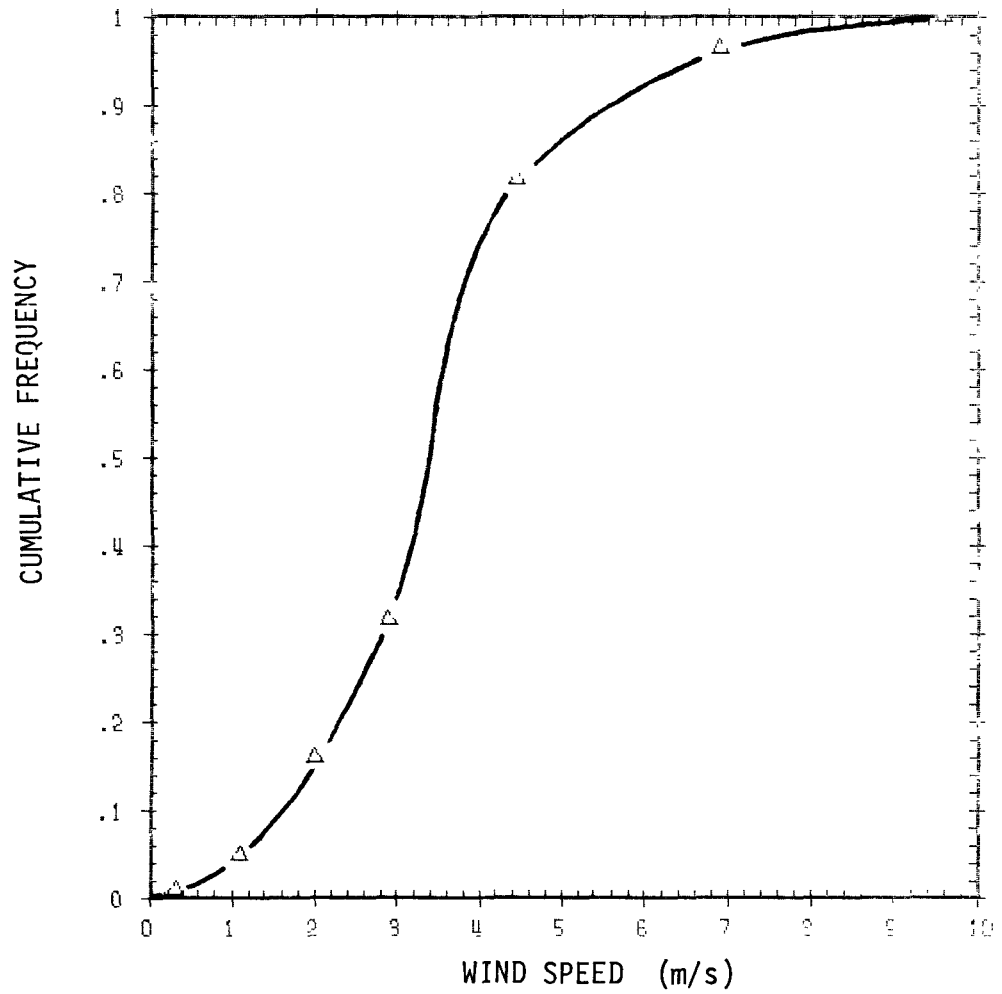


Figure 3. Cumulative frequency distribution of wind speeds for northwest winds under neutral stability (valley tower location).

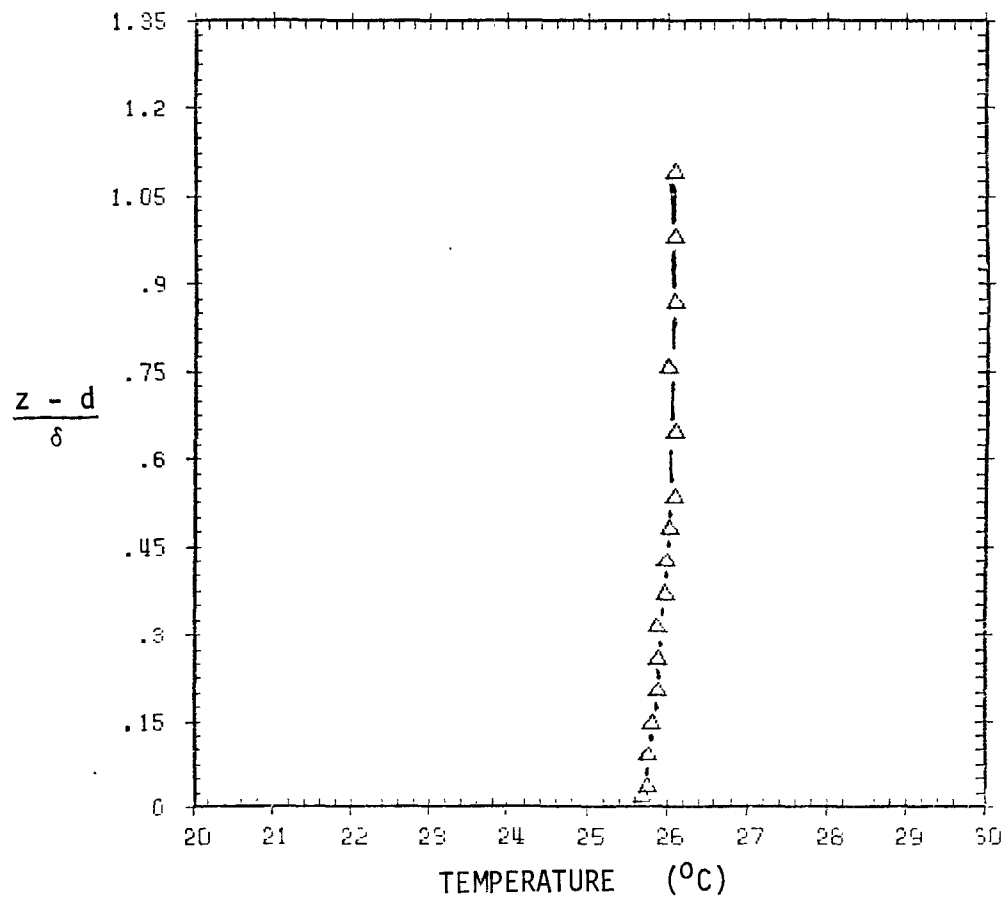


Figure 4. Vertical temperature profile in wind tunnel test section.

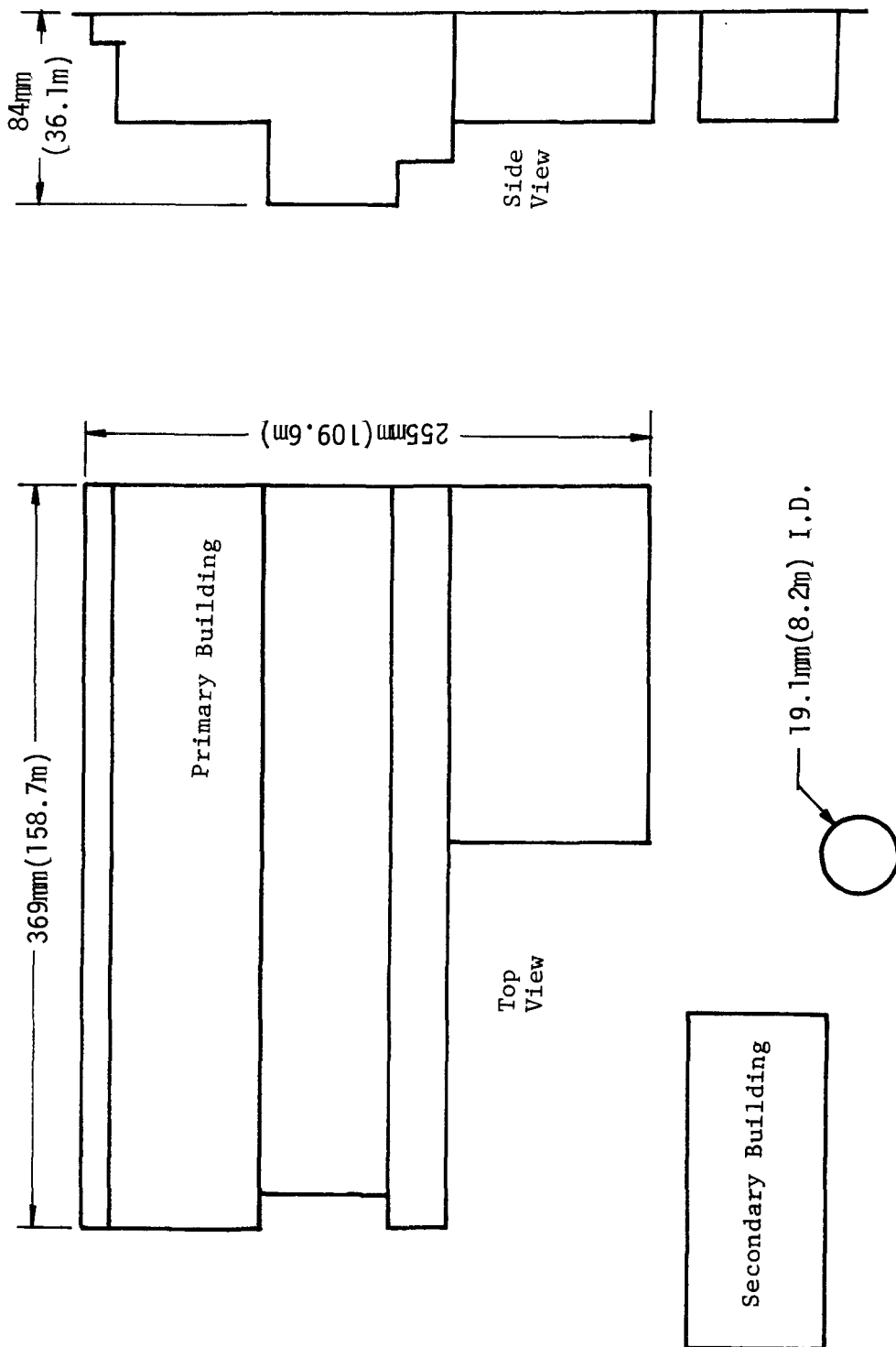


Figure 5. Top and side views of the building. (Full-scale dimensions shown in parentheses.)

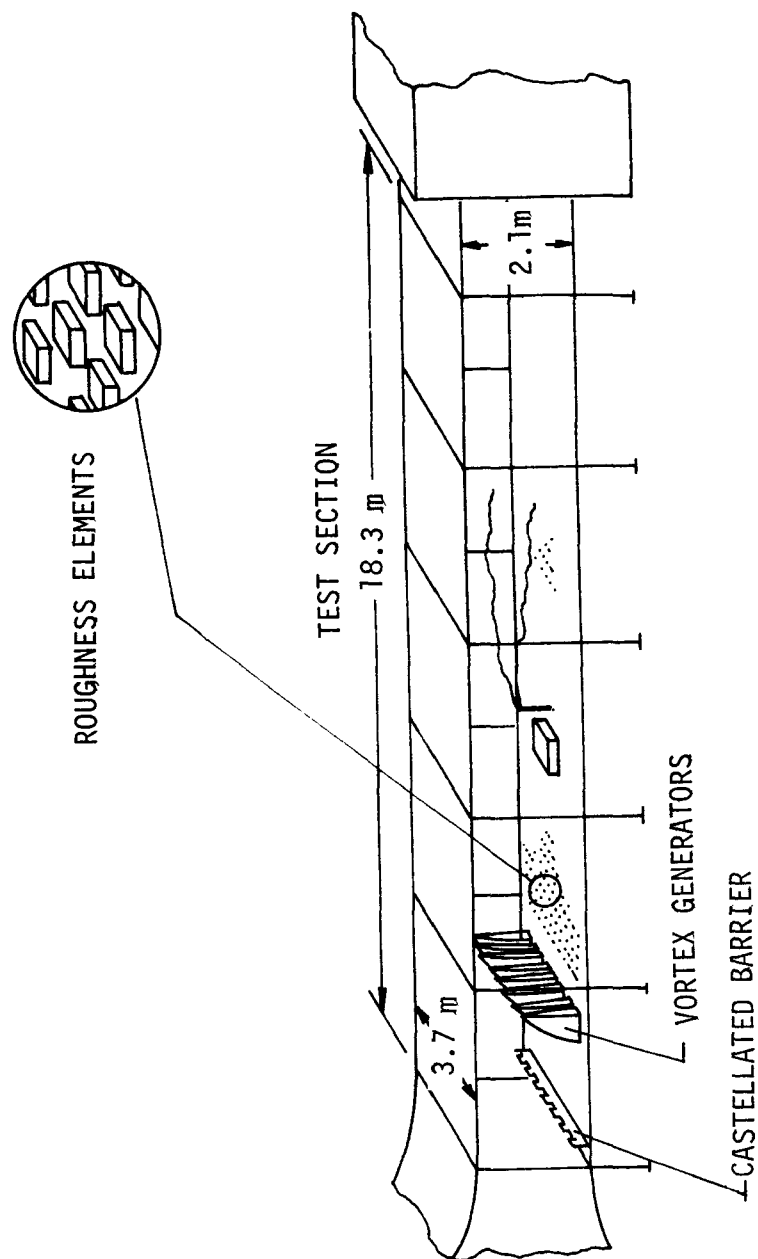


Figure 6. Schematic of the boundary-layer simulation system.

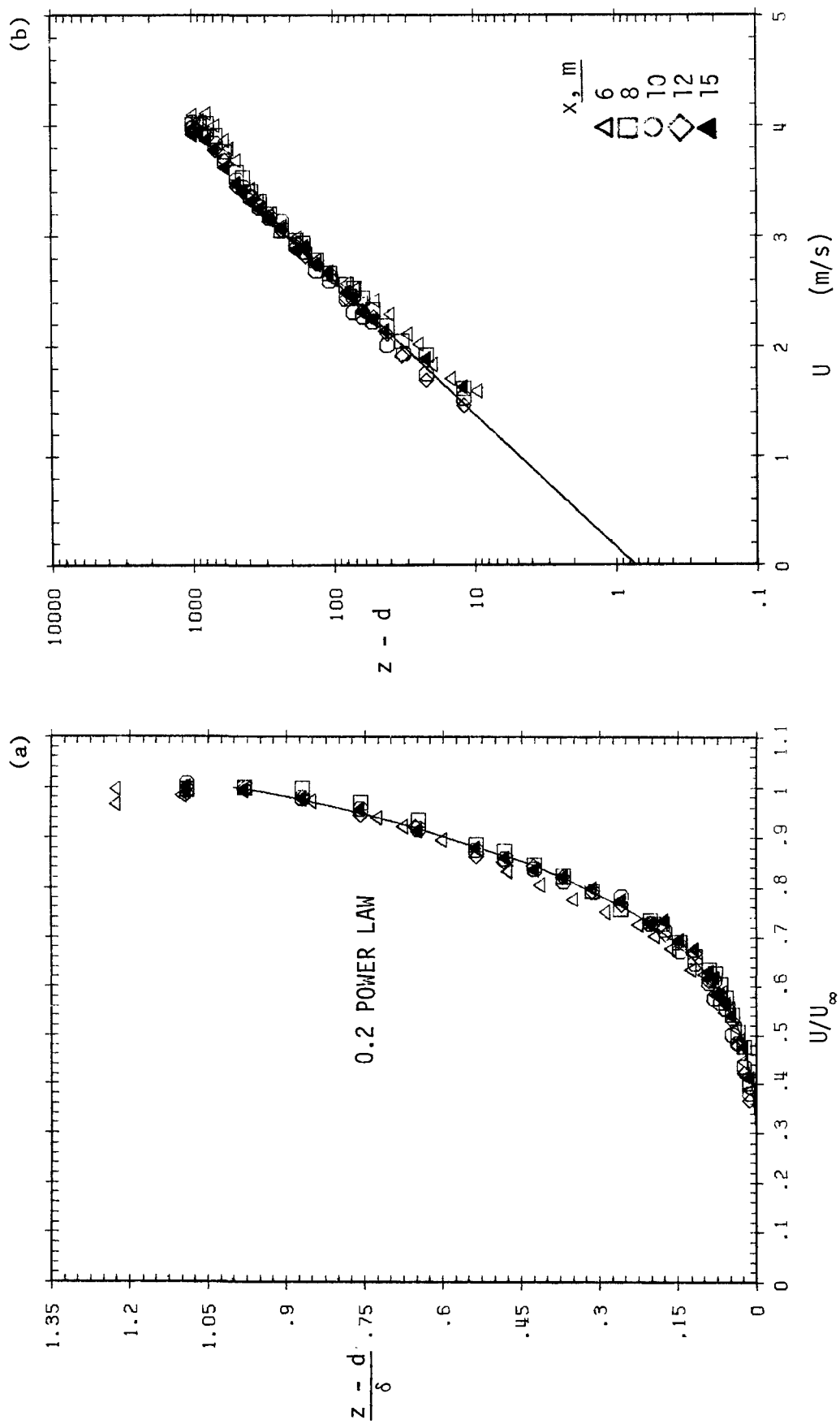


Figure 7. Velocity profiles for the simulated atmospheric boundary layer.

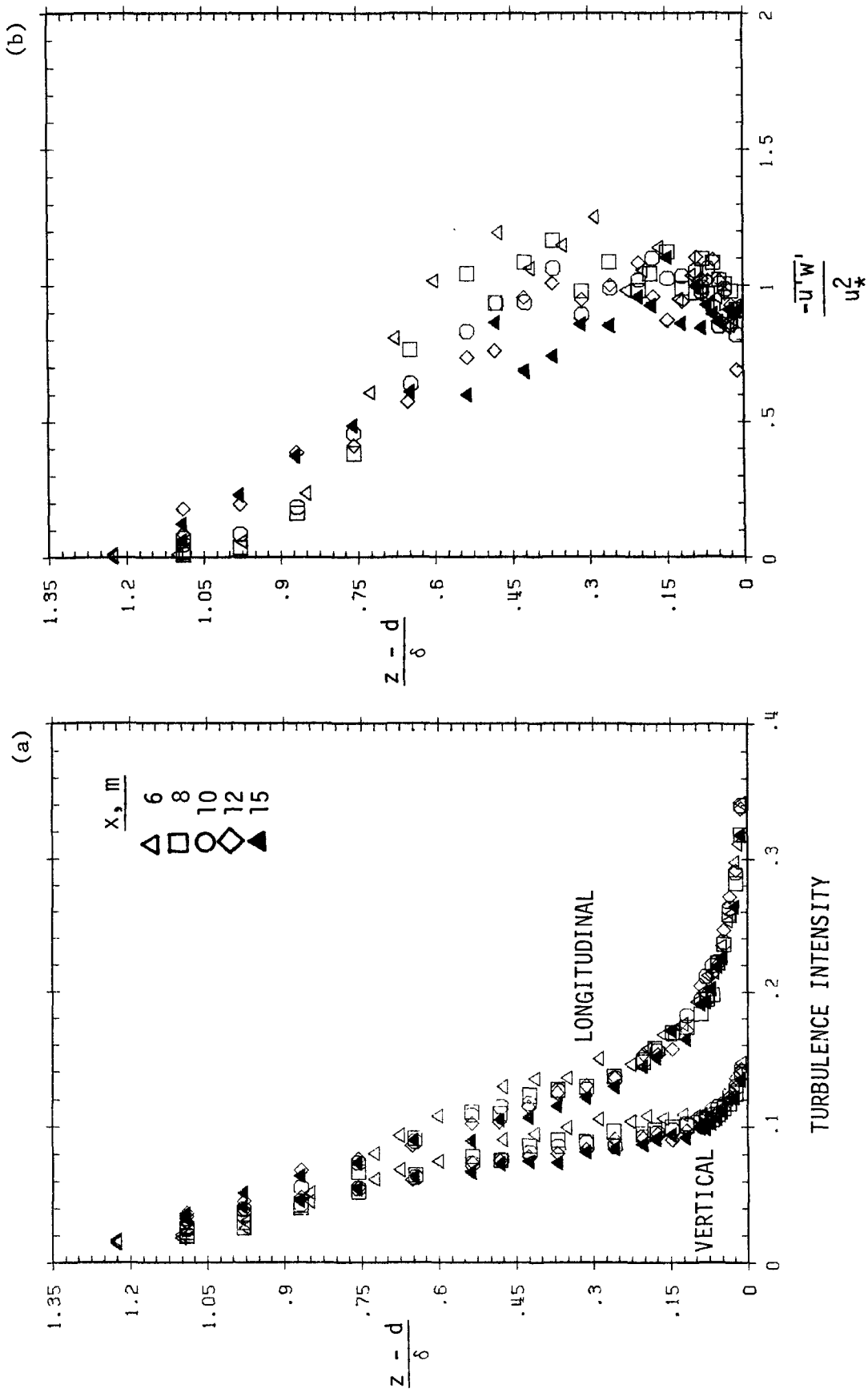


Figure 8. Turbulence intensity and Reynolds stress profiles.

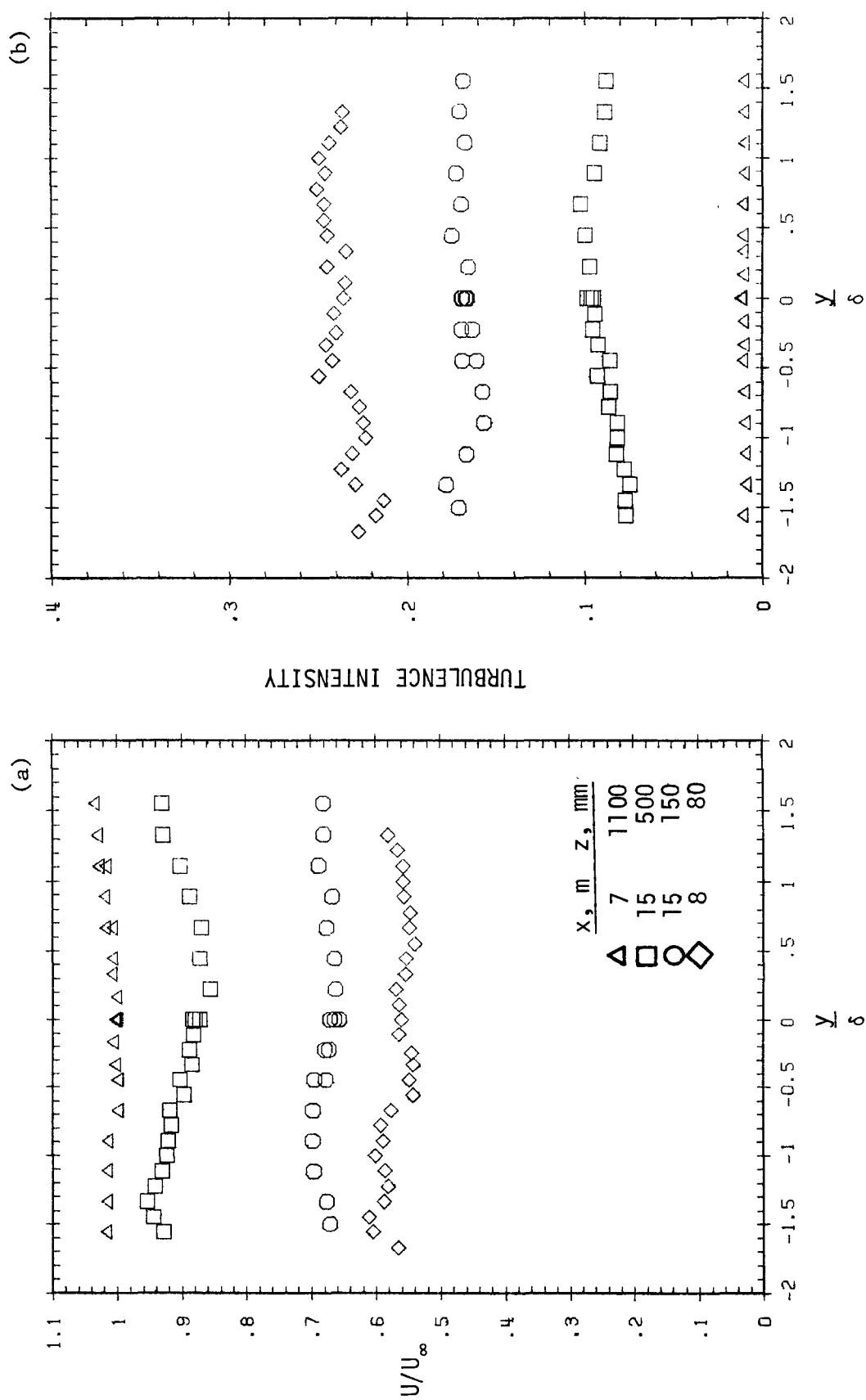


Figure 9. Lateral uniformity of (a) mean velocity and (b) longitudinal turbulence intensity.

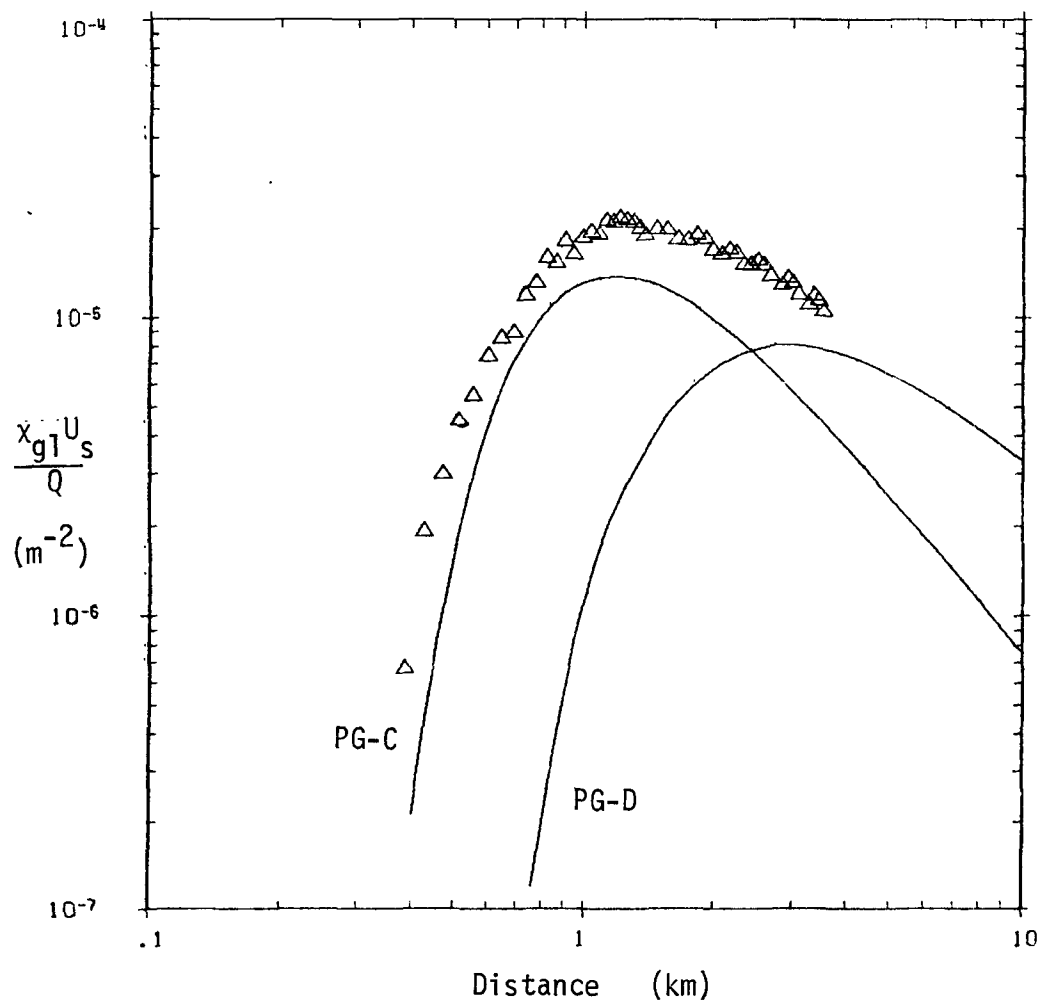


Figure 10. Surface concentration profiles (Δ) compared with Pasquill-Gifford C and D stability.

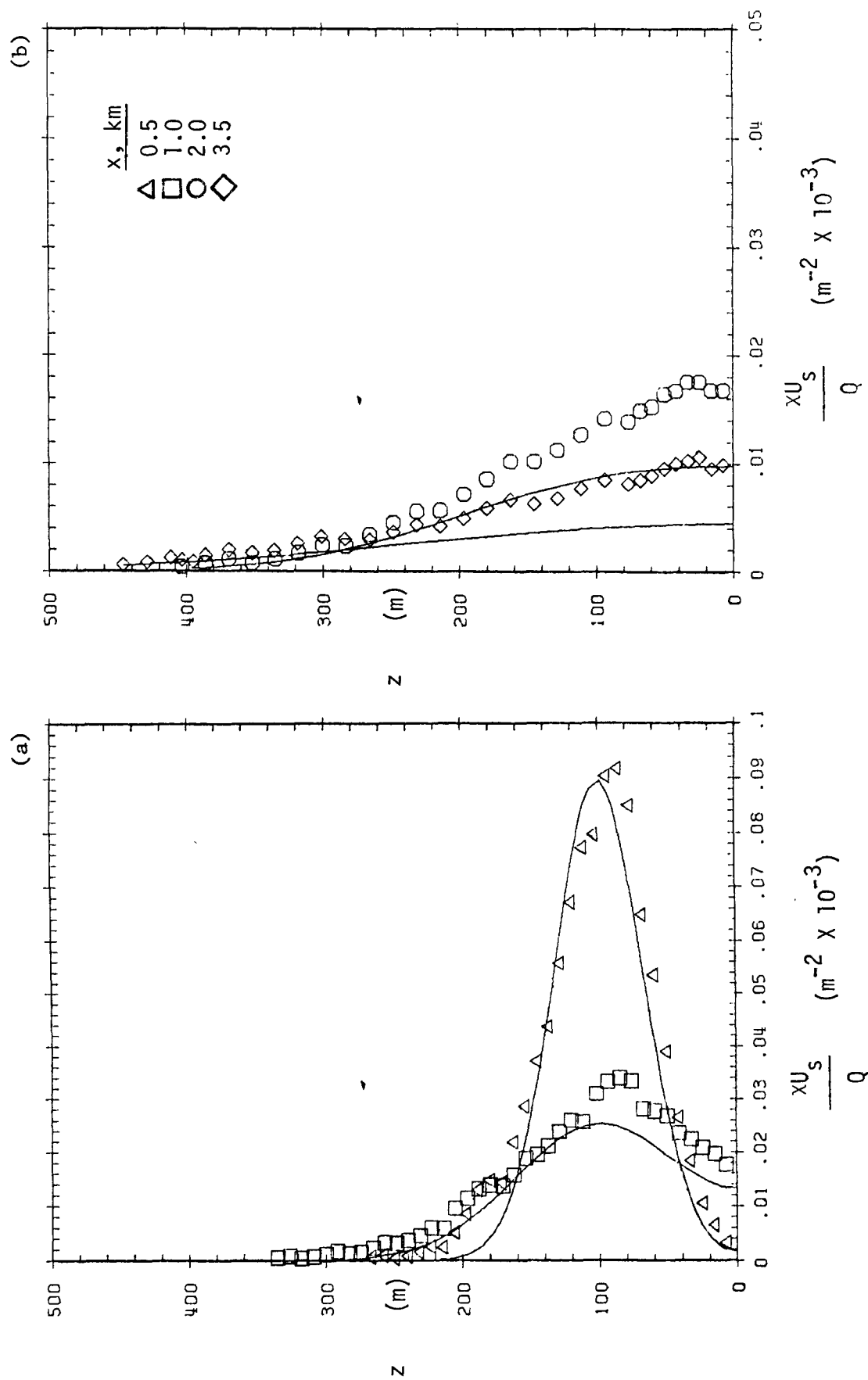


Figure 11. Vertical concentration profiles compared with Pasquill-Gifford C stability.

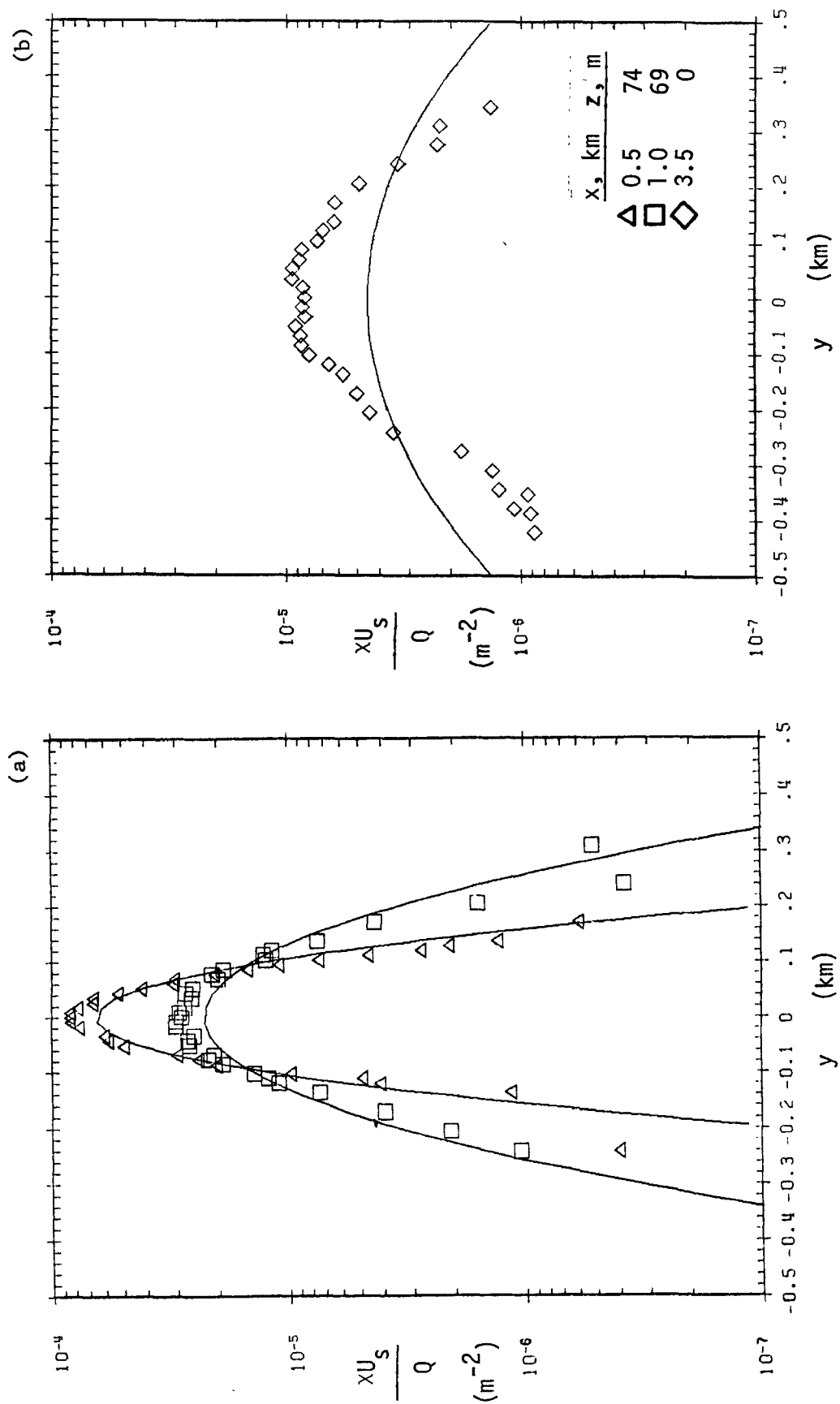


Figure 12. Lateral concentration profiles compared with Pasquill-Gifford C stability.

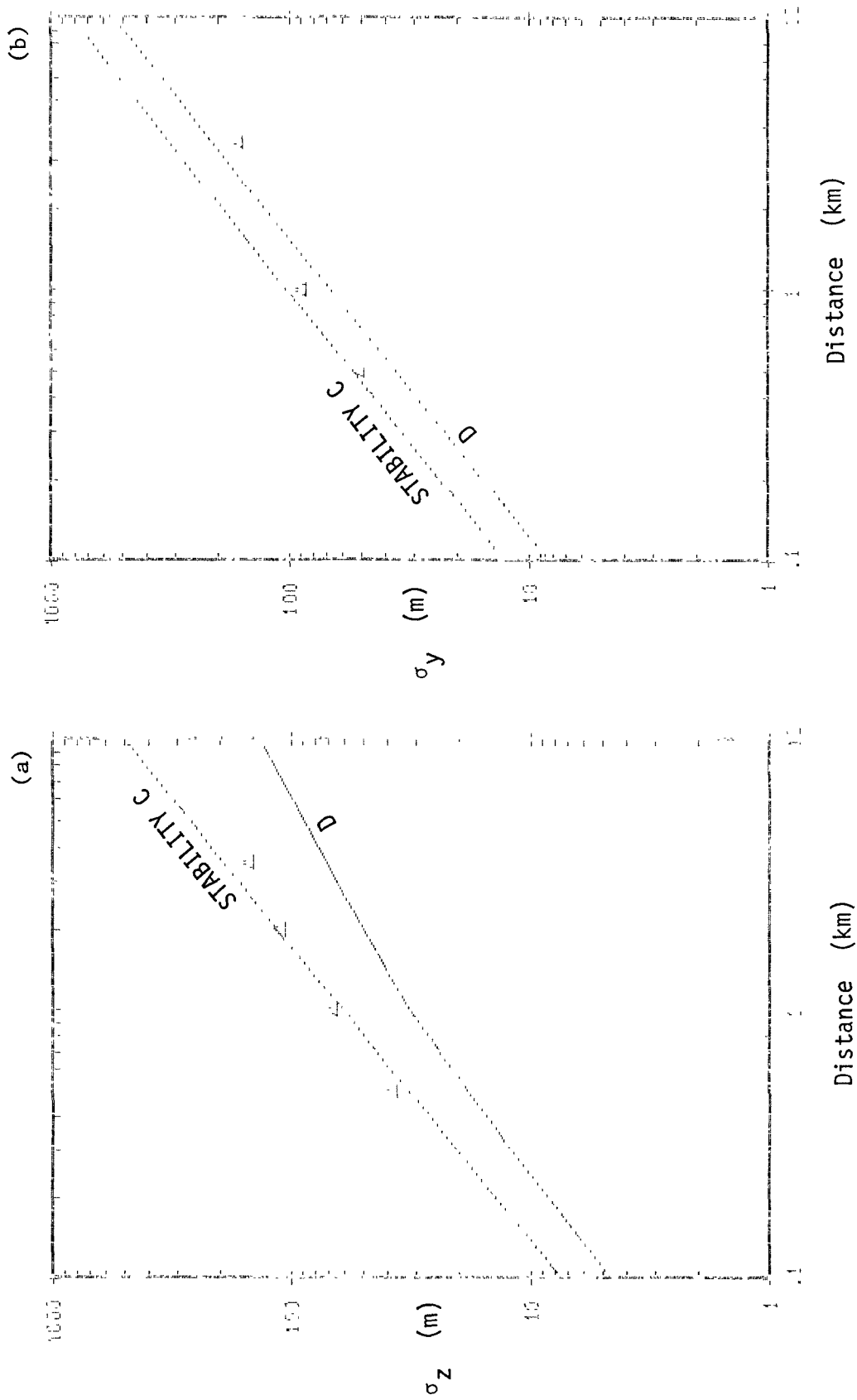


Figure 13. Plume widths compared with Pasquill-Gifford curves.

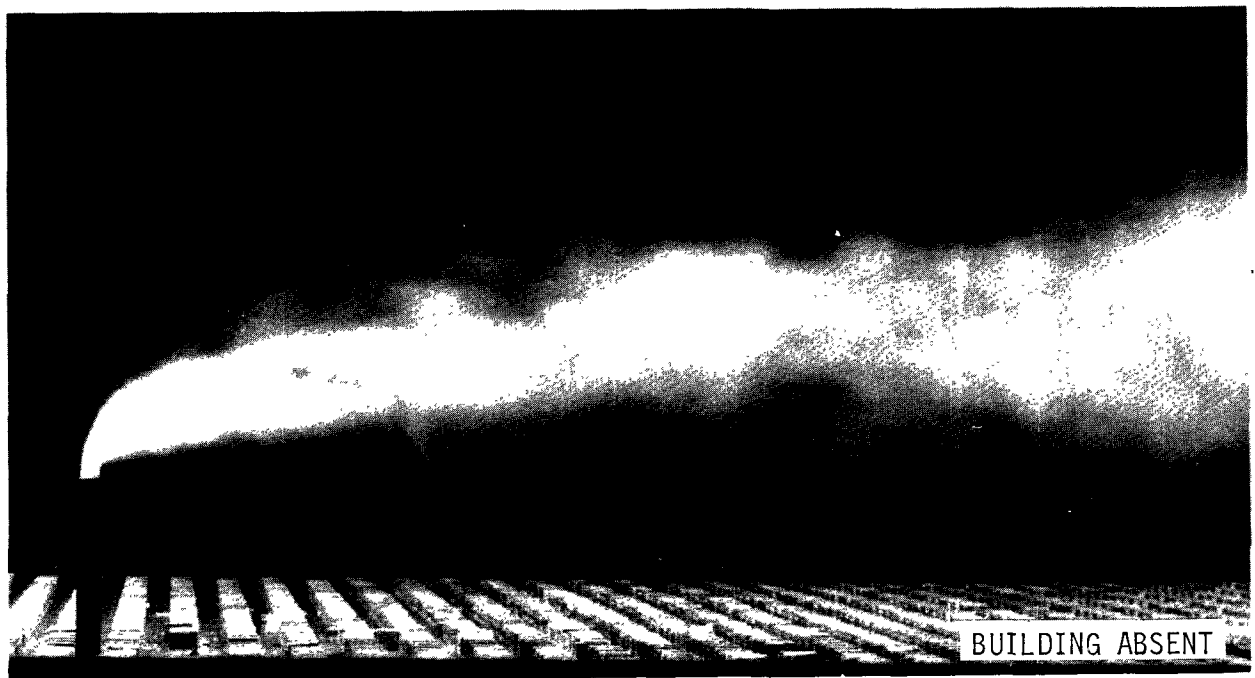
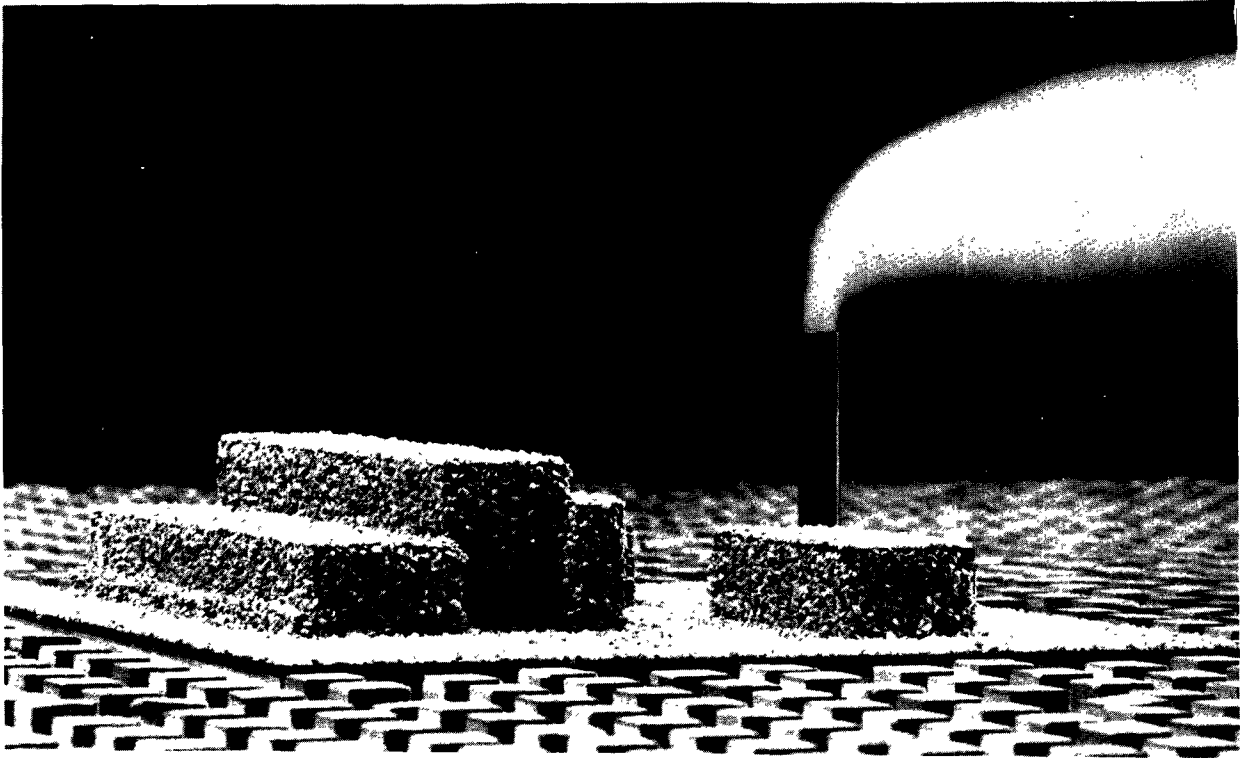


Figure 14. Flow visualization using paraffin-oil smoke source. $H_s = 64.1\text{m}$, 100% plant load.

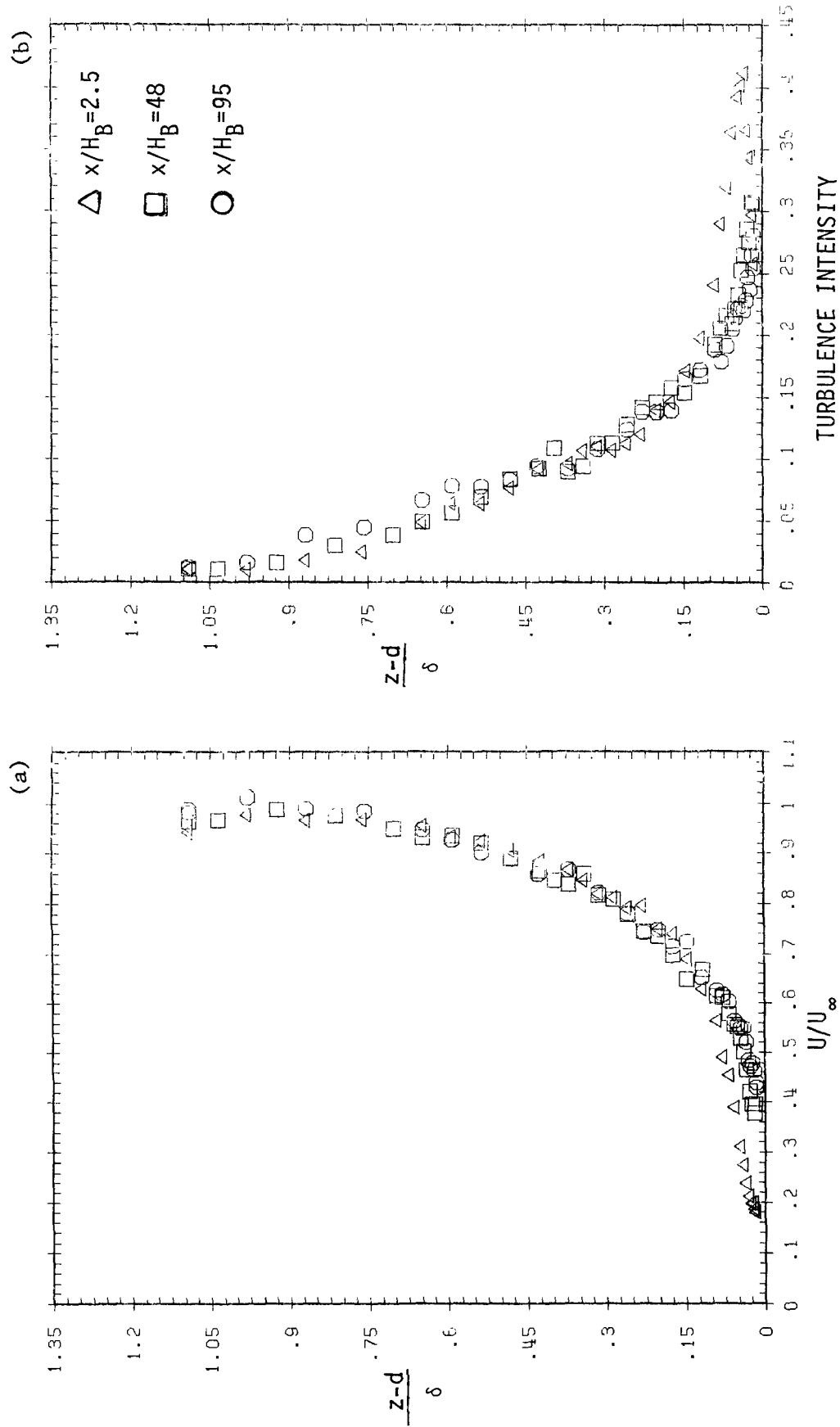


Figure 15. Vertical profiles of mean velocity and longitudinal turbulence intensity downstream of the model building.

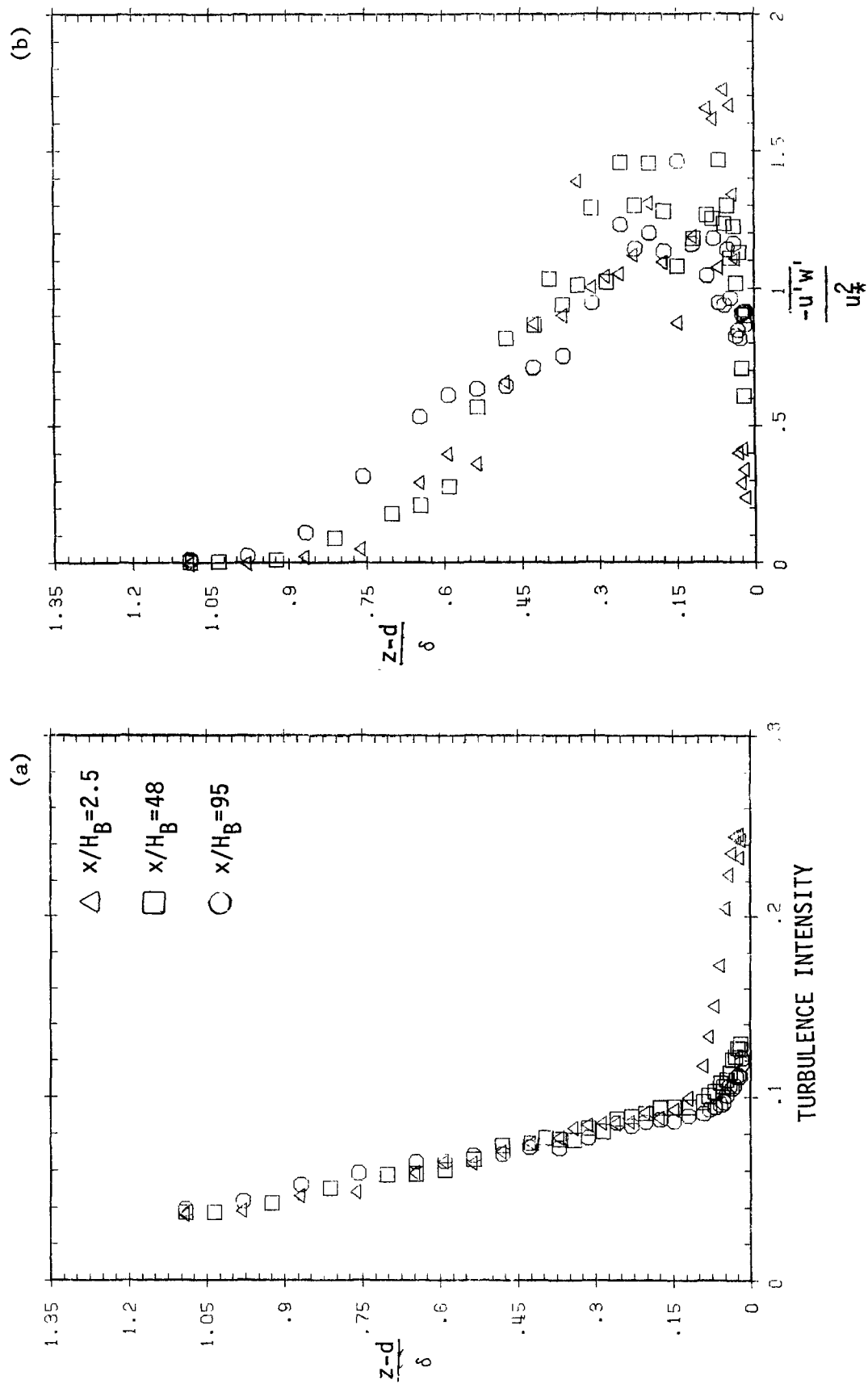


Figure 16. Vertical profiles of (a) vertical turbulence intensity and (b) Reynolds stress downstream of the model building.

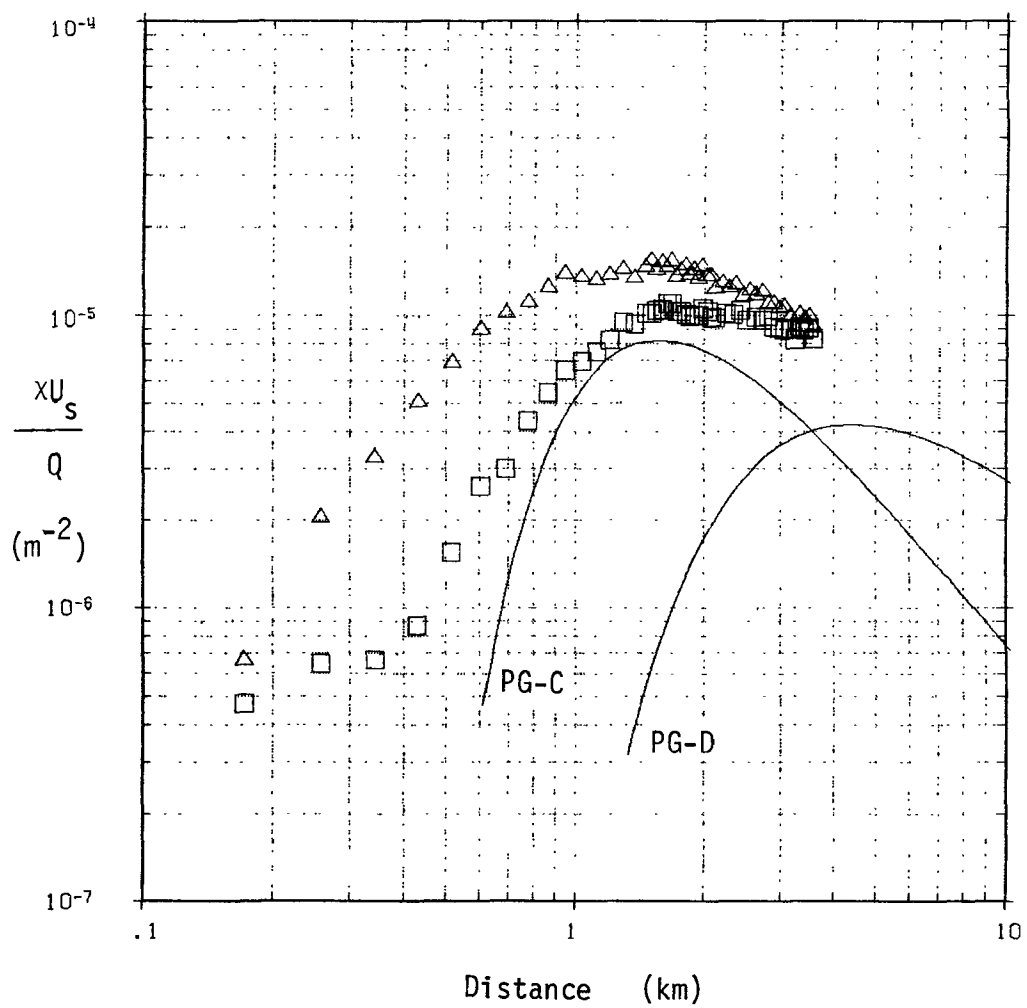


Figure 17. Surface concentration profiles with (Δ) and without (\square) the building. Stack height 64.1m.

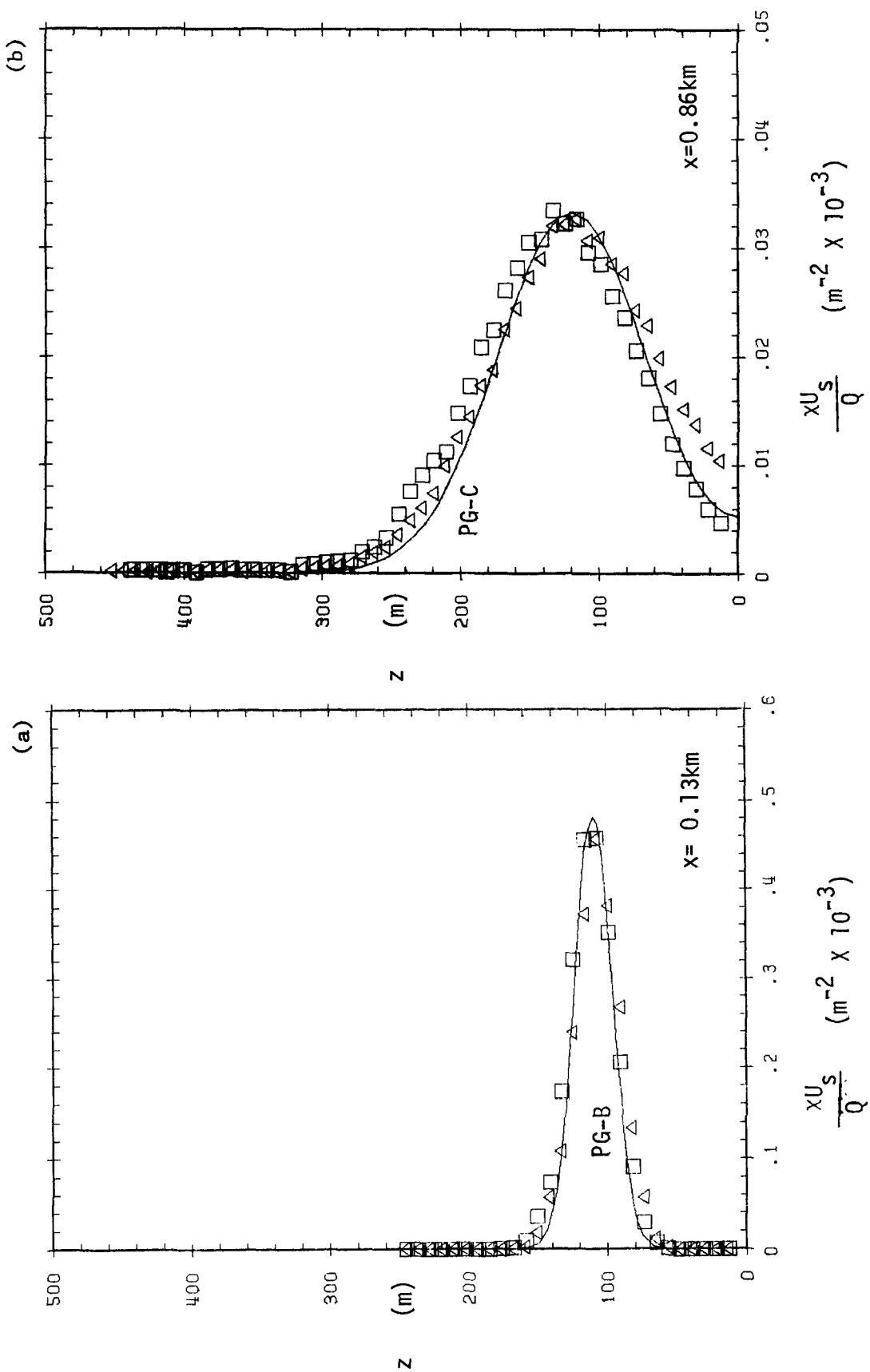


Figure 18. Vertical concentration profiles with (Δ) and without (\square) the building. Stack height 64.1m.

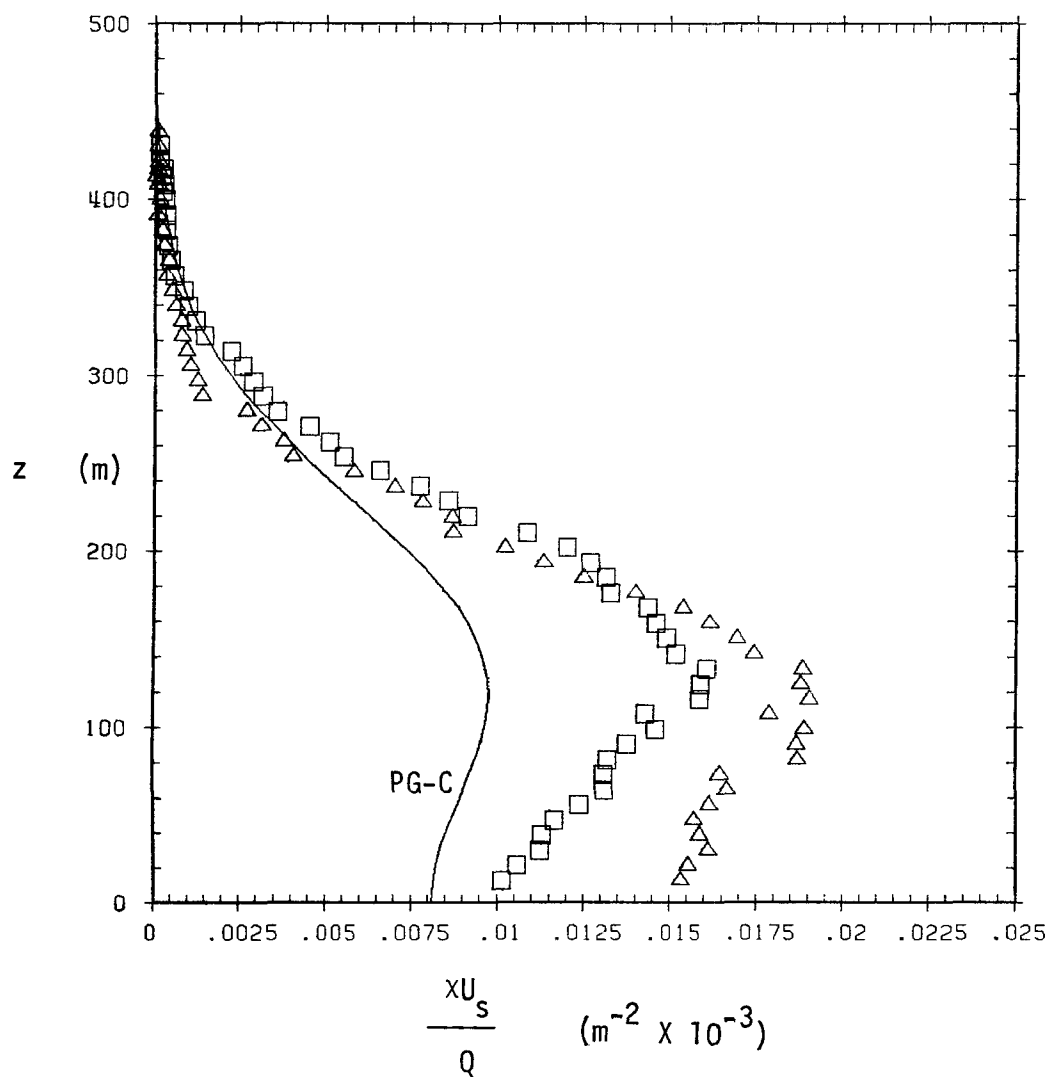


Figure 19. Vertical concentration profiles with (Δ) and without (\square) the building. Stack height 64.1m, downstream distances of 1.5km and 1.7km respectively.

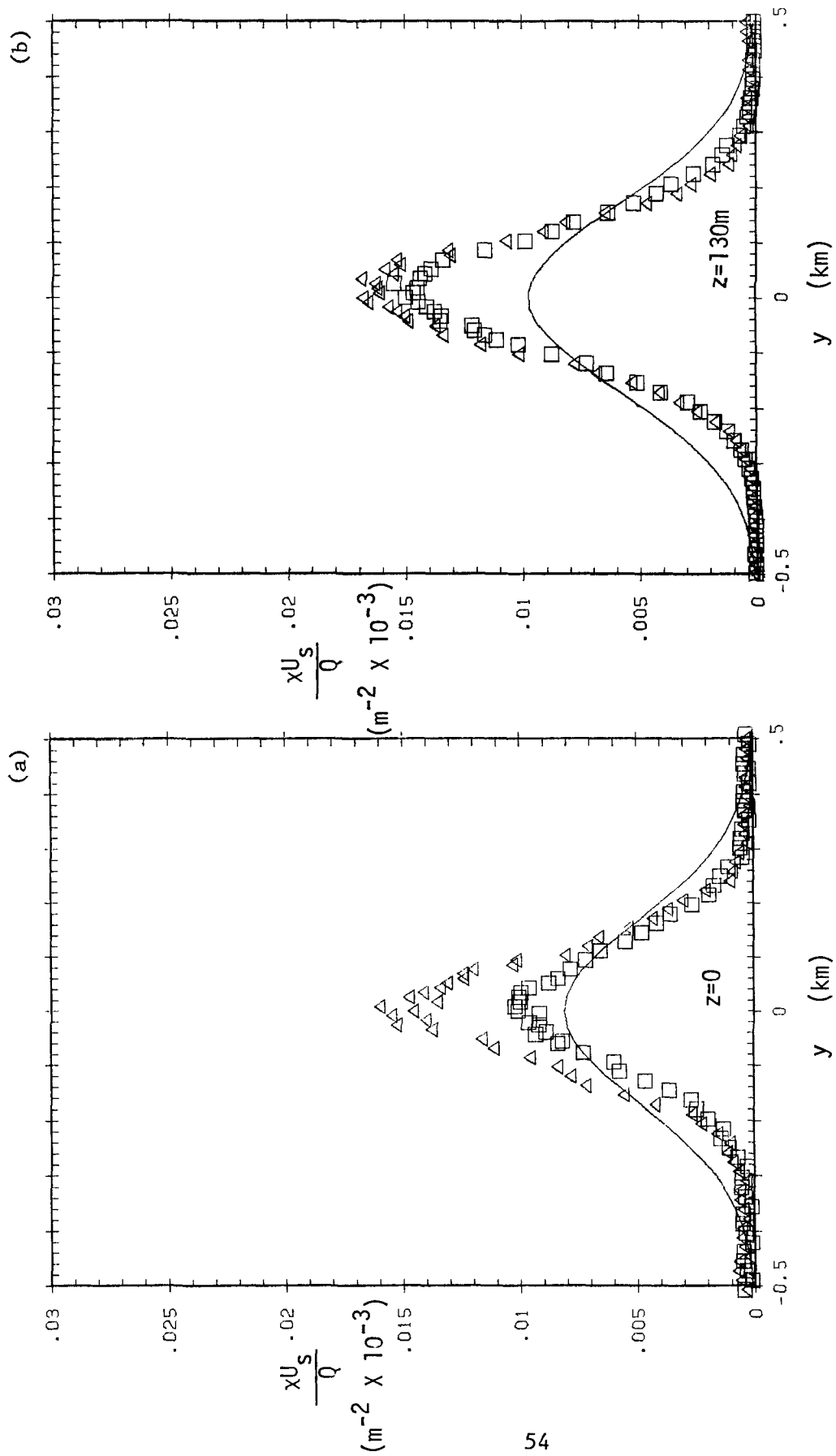


Figure 20. Lateral concentration profiles with (Δ) and without (\square) the building. Stack height 64.1m, downstream distances of 1.5km and 1.7km respectively.

APPENDIX A

DESCRIPTION OF FACILITIES AND INSTRUMENTATION

A.1 The Fluid Modeling Facility Wind Tunnel

This study was conducted in the Environmental Protection Agency's Meteorological Wind Tunnel. It is an ultra-low speed, open-return wind tunnel with a test section 2.1 m high, 3.7 m wide and 18.3 m long. Air enters the test section through a flow-straightening honeycomb and four turbulence-reducing screens. A plenum chamber just prior to the 2.8-to-1 contraction allows turbulence in the wake of the screens to decay. An adjustable ceiling allows compensation for blockage effects of models and achievement of a zero-pressure gradient in the test section. Transparent windows form the sides of the test section to facilitate flow visualization. An instrument carriage provides the capability for positioning a probe anywhere in the test section with an accuracy of ± 1 mm. Controls and readout for the carriage are conveniently located at an operator's console. After the test section, the air passes through an acoustic silencer, a rectangular-to-round transition section, the fan, a diffuser, and another acoustic silencer before being exhausted back into the room. The tunnel is driven by a 75 kilowatt AC motor with eddy-current coupler for speed control of the 1.8 m diameter fan. This apparatus provides steady speeds in the test section of 0.3 to 8 m/s. The motor and fan assembly is enclosed in an acoustic silencer to provide a low noise level in the laboratory. Further details of the wind tunnel and its operating characteristics are described by Snyder (1979b).

A.2 INSTRUMENTATION

A.2.1 Velocity measurements

Mean velocity, turbulence intensity, and shear-stress profile data were obtained with TSI, Inc. model 1054A constant-temperature anemometers in conjunction with model 1241-T1.5 x-array hot-wire probes (end-flow style). Calibrations were performed in the free-stream with the sensor mounted on the instrument carriage. The reference velocities for calibration were obtained with a Dwyer model 160-24 pitot-static tube; the differential pressure was monitored with an MKS Baratron capacitance manometer (model 310BH sensor head with model 170M electronics unit). Yaw calibrations of the sensors were performed in separate series of tests in an instrument calibration tunnel.

Temperature near the sensor location was monitored both during calibration and routine operation by a Hewlett-Packard model 2801A quartz thermometer. Analog output from the anemometers was converted to digital form by a 12 bit analog-to-digital converter. The resulting data were processed on a Digital Equipment Corp. PDP-11/40 minicomputer. Two-minute averages at a sampling rate of 1000 samples per second yielded reasonably stable mean values ($\pm 1\%$ on mean velocity). Further details of the hot-wire and data-processing systems are given by Snyder (1979b).

A.2.2 Concentration measurements

A hydrocarbon tracer technique was used to measure concentrations downwind of the source. The technique employed CP grade ethylene (minimum purity of 99.5 mole percent) as the tracer source. Concentrations were measured with Beckman model 400 flame ionization detectors (FIDs), operated in the continuous sampling mode.

The FIDs were calibrated using 1% certified (Scott Environmental Technology, Inc.) "span" gas; zeroing was accomplished with "zero" air (< 1 ppm hydrocarbons). The FIDs were shown in a separate series of tests to be linear over four decades of concentration (Khurshudyan et al, 1981). The samples to be analyzed were drawn from a "rake" of tubes which was mounted on the instrument carriage to allow convenient positioning. The sample flow rate was 200 cm³/min. Five analyzers were used simultaneously to speed the process of acquiring data. One of the five constantly monitored background concentration upstream of the source. Analog output from the FIDs was also digitized to 12-bit precision for processing by the minicomputer.

A.2.3 Data acquisition system

All laboratory data were collected using a Digital Equipment Corp. PDP-11/40 minicomputer. Anemometer calibrations were performed over the velocity range of interest (typically 6 to 9 points over the range 1 to 5 m/s). During calibration, the computer was used to fit a King's Law form of equation to the calibration data. This best fit relation was then used to generate a "look-up" table for conversion of voltage to velocity during routine operation. A typical calibration curve is shown Figure A-1. The hot-wire anemometer was typically sampled at 1000 samples per second, and data reduction took place between samples; hence, real-time outputs of velocity, intensity, and shear stress were available. Temperature compensation was accomplished using the method of Bearman (1971), which required occasional modification of the look-up table as temperature in the test section (room temperature) changed.

As the time constant of the FIDs is on the order of 0.5 second, these

units were sampled at a rate of one sample per second. Two-minute averages again provided stable mean values. The FIDs have linear response, so that the generation of mean values was straightforward. Zero and span values were recorded at the beginning and end of each test to assure that analyzer drift was not a problem. Background values were subtracted from each sample to account for background drift.

All data files were stored on disk for later processing and preserved on magnetic tape.

A.2.4 Volume flow measurements

Ethylene, helium and air were mixed prior to injection into the model stack in order to obtain correct density and velocity ratios. The flow rates of these gases were measured and continuously monitored using Meriam laminar-flow elements (LFEs); the differential pressure was observed on Meriam micromanometers. Figure A-2 shows the typical apparatus for injecting gases into the tunnel. Calibration of the LFEs was accomplished using a volumetric flow calibrator (Brooks model 1050A 1J1), which had a rated accuracy of 1/2%. Where significant back-pressures were anticipated, as for example, with the porous ball stack, the back-pressure was monitored as a check on system integrity.

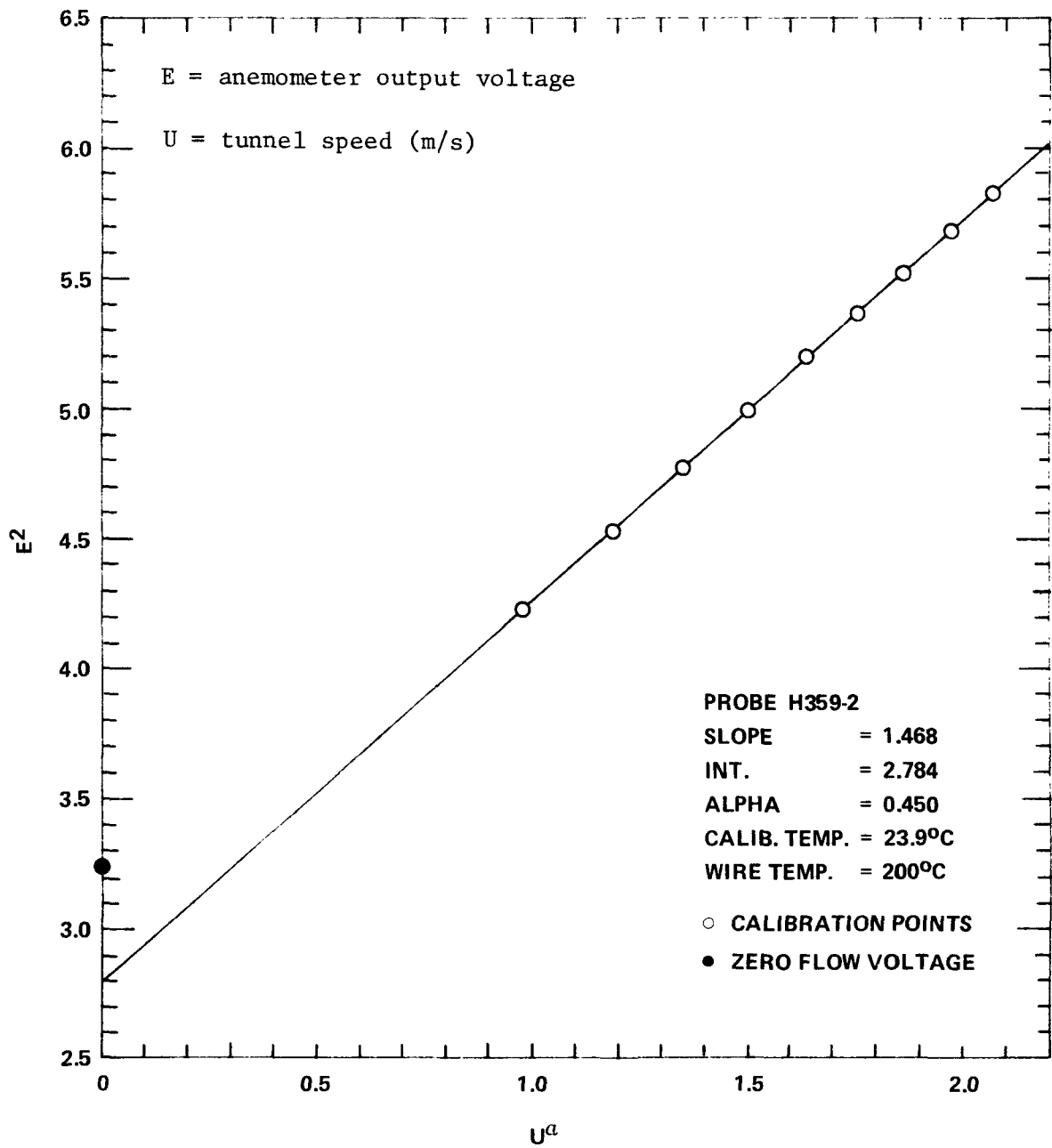


Figure A1. Typical calibration curve for hot-wire anemometer.

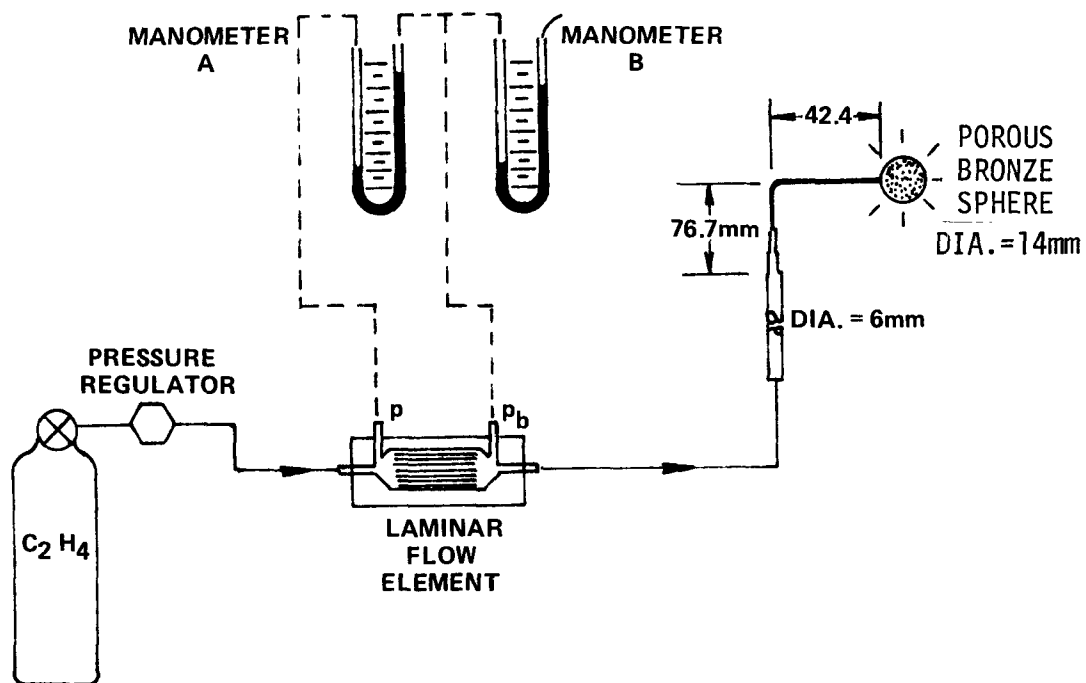


Figure A2. Diagram of source and flow measurement apparatus used for dispersion comparability test.

APPENDIX B
CONCENTRATION MEASUREMENTS FOR STACK HEIGHTS OF
54.2m, 68.8m, 72.3m, AND 90.3m

Figures B1 through B4 present the concentration measurements made over a range of stack heights for the purpose of initially determining the appropriate GEP stack height. The measurements were carried out in the same manner as those for the GEP stack height described in sections 6.1 and 6.2. Note that the effluent-to-wind-speed ratio differs slightly for each stack height presented. Figure B5 shows the results of these measurements in terms of percent excess concentration versus stack height, where excess concentration is defined as the ratio of the maximum ground-level concentration with the building to the maximum ground-level concentration in the absence of the building minus one.

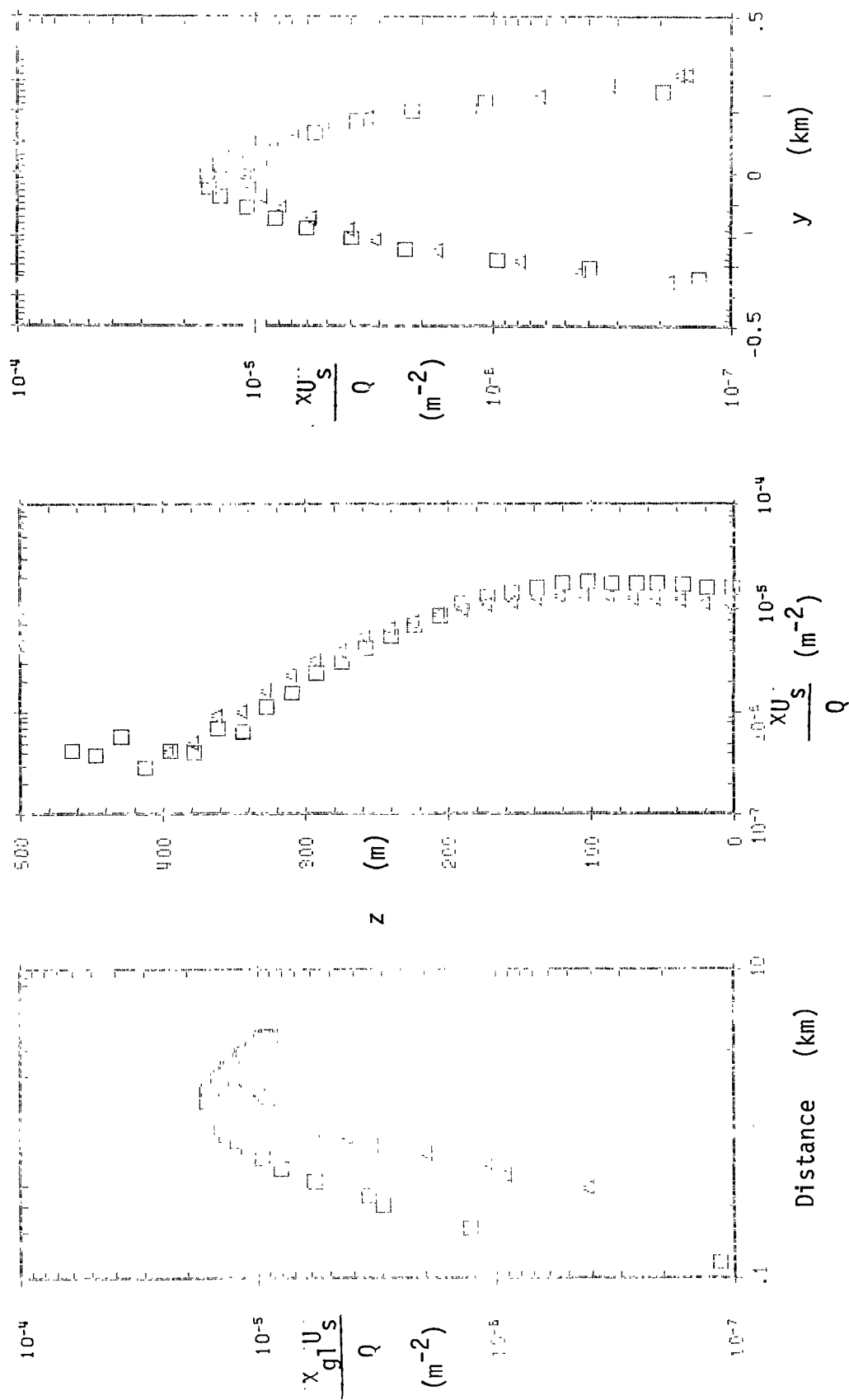


Figure B1. Concentration profiles with (\square) and without (Δ) the building.
Stack height 54.2m, 100% plant load, $W/U_s=3.60$.

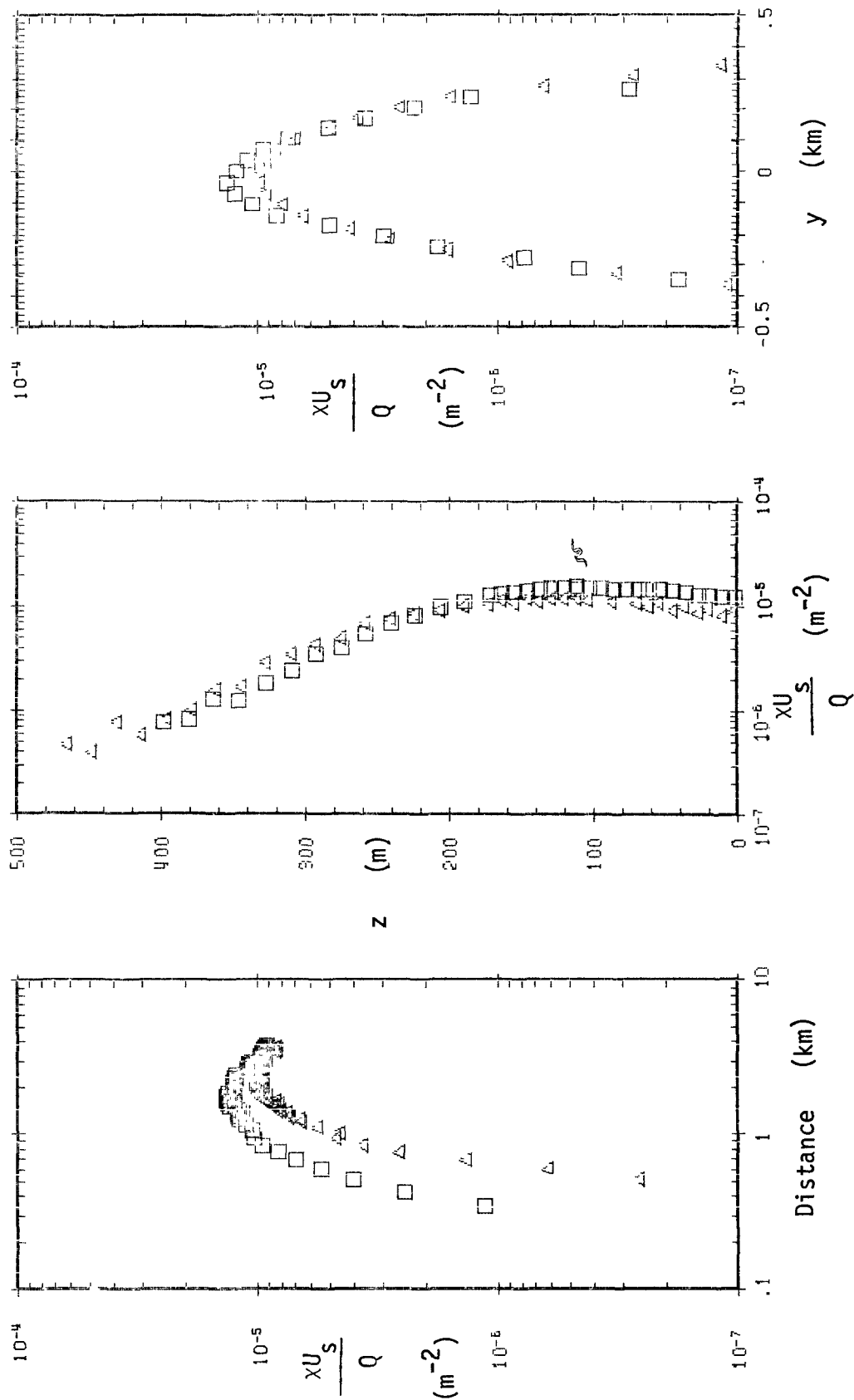


Figure B2. Concentration profiles with (\square) and without (Δ) the building.
Stack height 68.8m, 100% plant load, $W/U_s=3.42$.

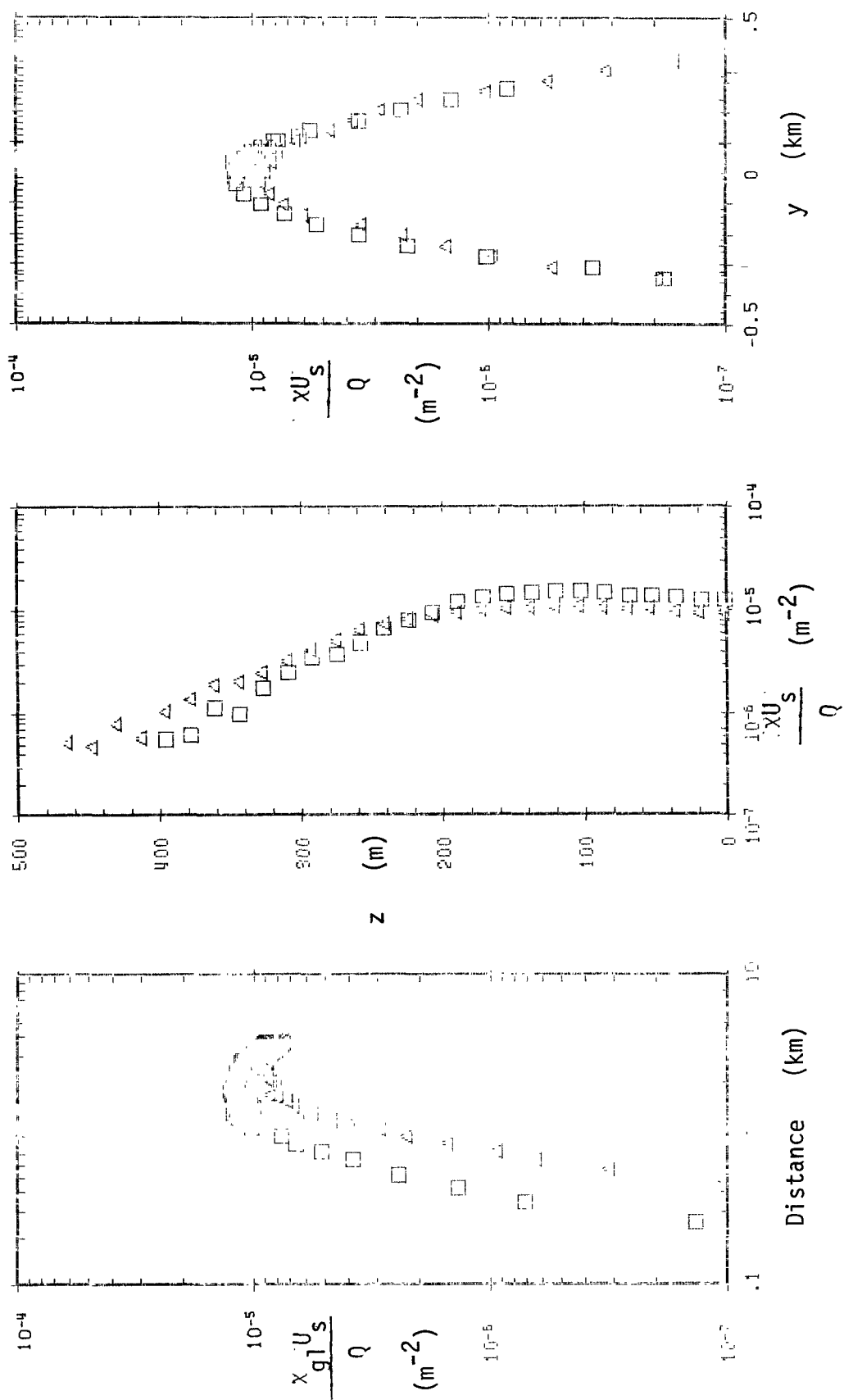


Figure B3. Concentration profiles with (\square) and without (Δ) the building.
Stack height 72.3m, 100% plant load, $W/U_s = 3.38$.

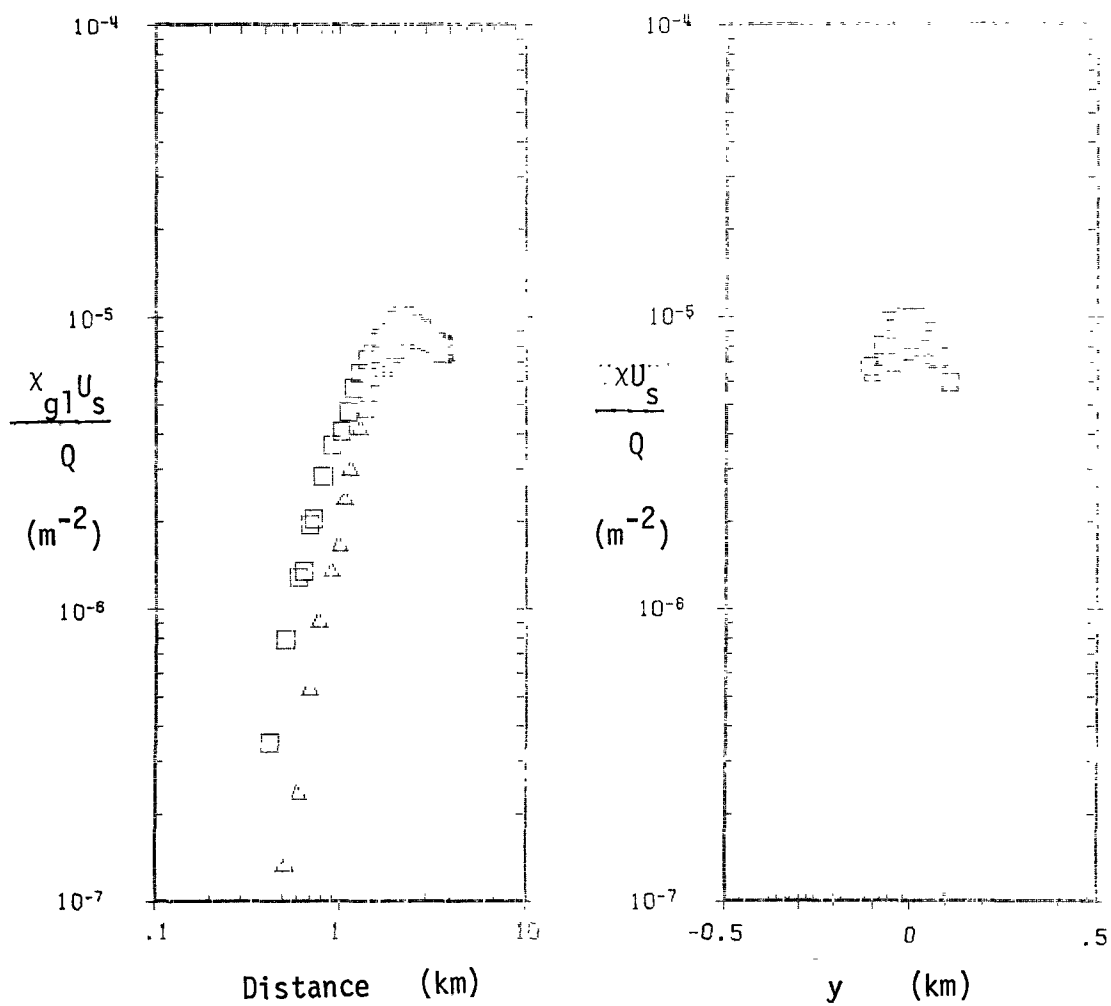


Figure B4. Concentration profiles with (\square) and without (\triangle) the building. Stack height 90.3m, 100% plant load, $W/U_s=3.22$.

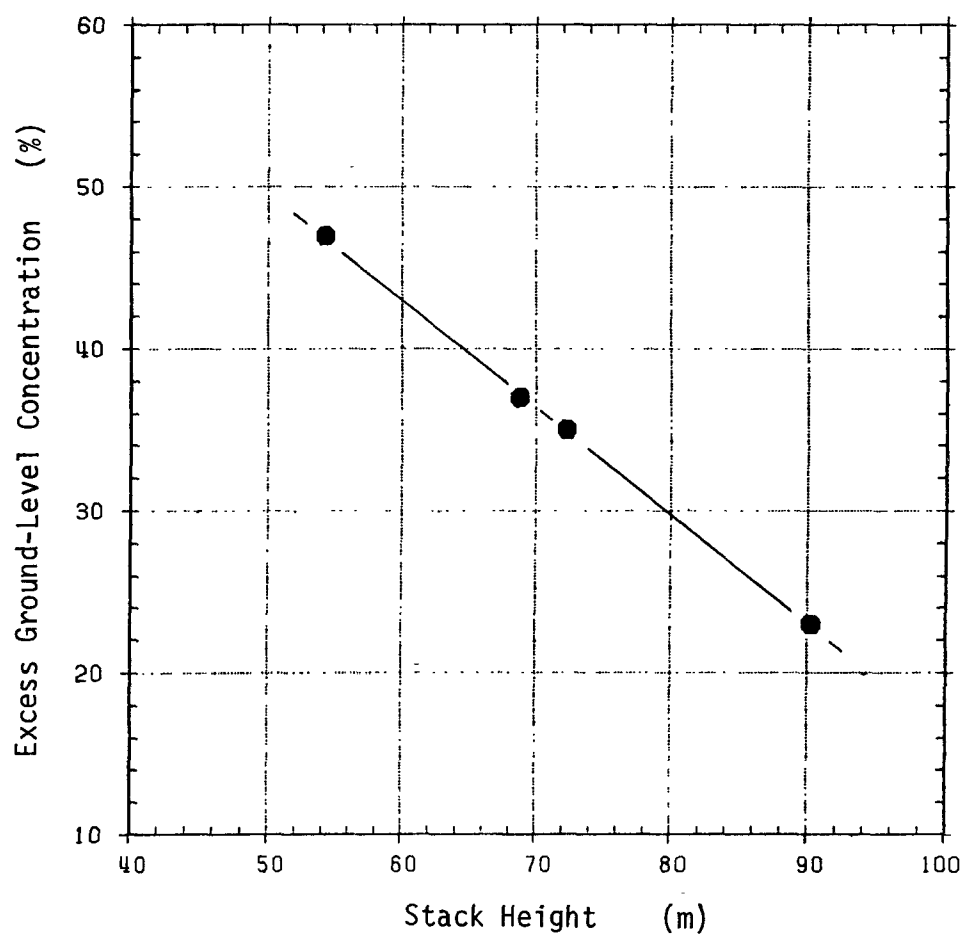


Figure B5. Percent excess ground-level concentration vs. stack height for 100% plant load conditions.

APPENDIX C

GEP STACK HEIGHT FOR 50% PLANT LOAD CONDITIONS

As described in section 6.3, a direct application of the working rule for GEP stack height indicates an expected value of 90.3 m or 2.5 building heights as compared with the experimentally obtained value of 64.1 m or 1.8 building heights. Two reasons were suggested for this difference: the large effluent-to-wind-speed ratio, and the location of the source relative to the building. While the location of the source relative to the building is fixed, the effluent-to-wind-speed ratio varies with plant load. This means that a determination of GEP stack height at reduced plant load would provide an indication of the sensitivity of GEP stack height to the effluent-to-wind-speed ratio. To pursue this idea, experiments were undertaken to determine the excess concentration appropriate to a stack height of 90.3 m and 50% plant-load conditions. The experimental arrangement was identical to that used for 100% plant-load conditions, except that the effluent-to-wind-speed ratio was reduced by one-half. This provided an effluent-to-wind-speed ratio for the 90.3-m stack of 1.61. The resulting measurements are shown as figures C1 and C2. The excess concentration in the presence of the building is approximately 35%. This value is consistent with other investigations, and therefore lends support to the rather low GEP stack height determined for 100% plant-load conditions.

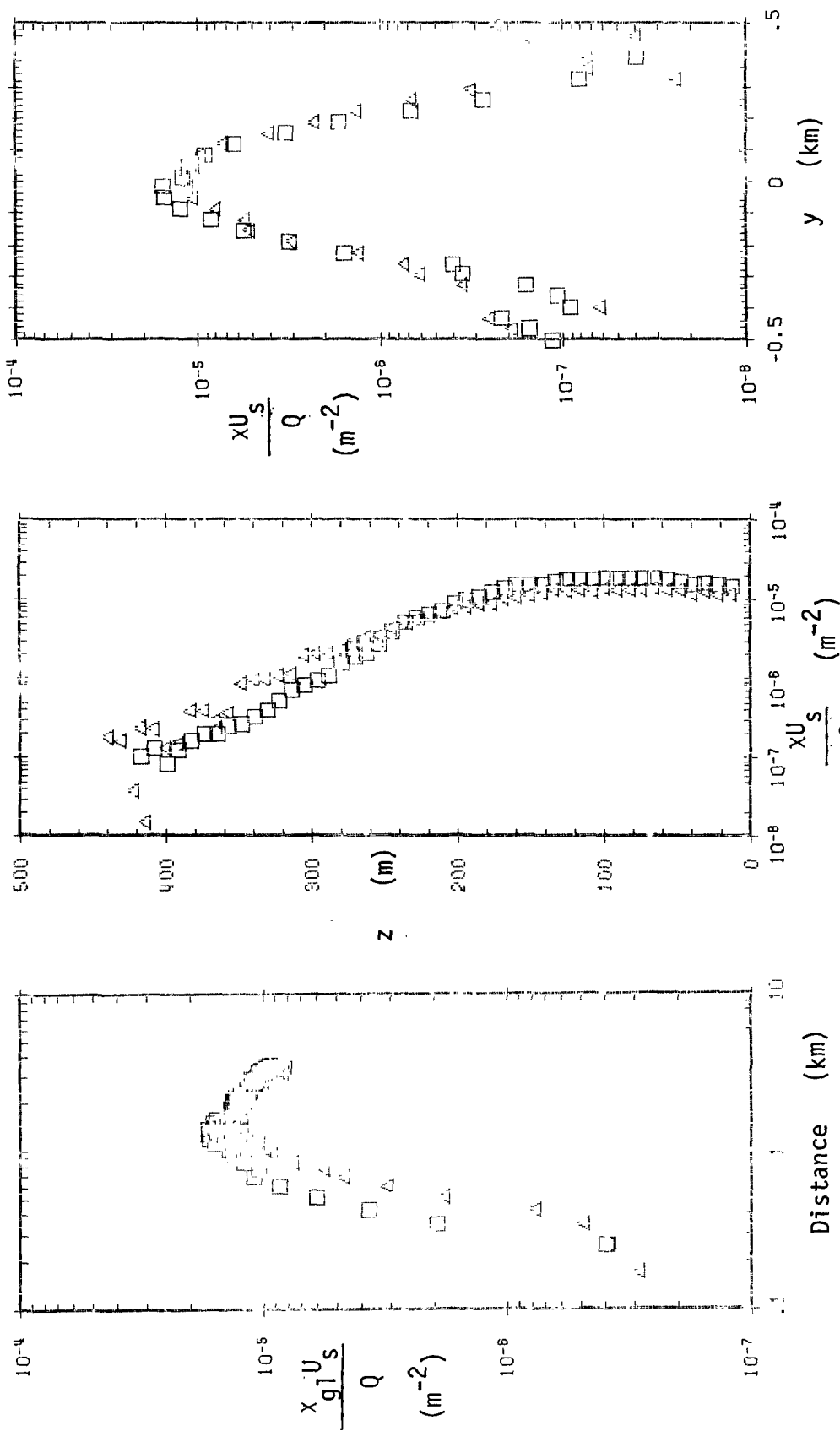


Figure C1. Concentration profiles with (\square) and without (\triangle) the building. Stack height 90.3m, 50% plant load.

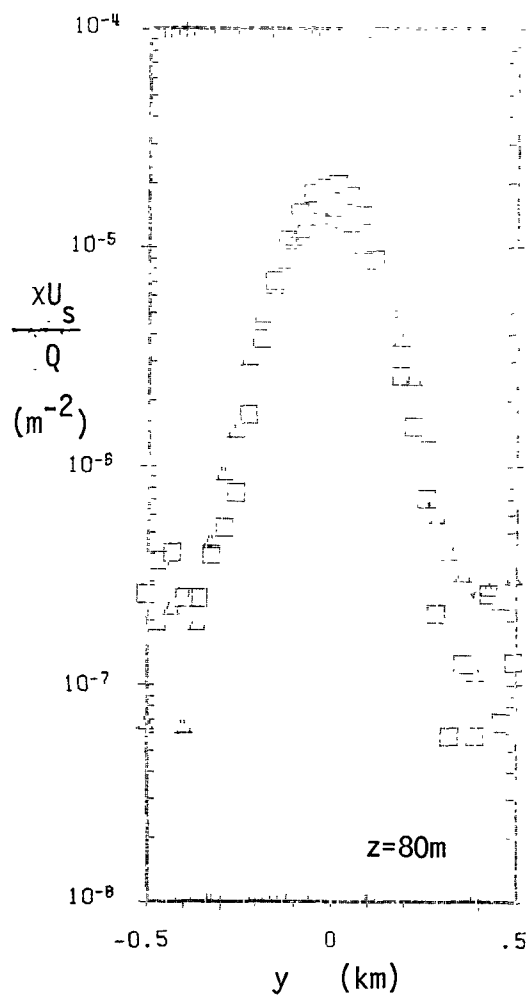


Figure C2. Concentration profiles with (\square) and without (\triangle) the building. Stack height 90.3m, 50% plant load.

APPENDIX D

RAW DATA LISTINGS

In order to reduce printing costs, the raw data listings have not been included with this report. Listings of the raw data are available from the authors on request.

TECHNICAL REPORT DATA
(Please read Instructions on the reverse before completing)

1. REPORT NO.	2.	3. RECIPIENT'S ACCESSION NO.
4. TITLE AND SUBTITLE DETERMINATION OF GOOD-ENGINEERING-PRACTICE STACK HEIGHT A Fluid Model Demonstration Study for a Power Plant		5. REPORT DATE
6. AUTHOR(S) Robert E. Lawson, Jr. ¹ and William H. Snyder ¹		7. PERFORMING ORGANIZATION CODE
8. PERFORMING ORGANIZATION NAME AND ADDRESS Environmental Sciences Research Laboratory Office of Research and Development U.S. Environmental Protection Agency Research Triangle Park, NC 27711		9. PERFORMING ORGANIZATION REPORT NO.
10. SPONSORING AGENCY NAME AND ADDRESS Environmental Sciences Research Laboratory -- RTP, NC Office of Research and Development U.S. Environmental Protection Agency Research Triangle Park, NC 27711		11. PROGRAM ELEMENT NO. CDTAlD/02-1313 (FY-83)
		12. CONTRACT/GRANT NO.
		13. TYPE OF REPORT AND PERIOD COVERED
		14. SPONSORING AGENCY CODE EPA 600/09
15. SUPPLEMENTARY NOTES 1. On assignment to the Environmental Protection Agency from the National Oceanic and Atmospheric Administration, US Department of Commerce		

16. ABSTRACT A study using fluid modeling to determine good-engineering-practice (GEP) stack height for a power plant installation is discussed. Measurements are presented to describe the simulated boundary layer structure, plume dispersion characteristics in the absence of the model plant building, and the maximum ground-level concentration of effluent downstream of the source, both with and without the model plant building. Analysis of the maximum ground-level concentration shows that, in this case, a stack height of 64.1m meets the current GEP criteria for 100% plant load conditions.		
--	--	--

KEY WORDS AND DOCUMENT ANALYSIS

DESCRIPTORS	b. IDENTIFIERS/OPEN ENDED TERMS	c. COSATI Field/Group
DISTRIBUTION STATEMENT RELEASE TO PUBLIC	19. SECURITY CLASS (This Report) - UNCLASSIFIED	21. NO. OF PAGES
	20. SECURITY CLASS (This page) UNCLASSIFIED	22. PRICE

U.S. ENVIRONMENTAL PROTECTION AGENCY

Office of Research and Development
Center for Environmental Research Information

Cincinnati, Ohio 45268

OFFICIAL BUSINESS

PENALTY FOR PRIVATE USE \$300
AN EQUAL OPPORTUNITY EMPLOYER

POSTAGE AND FEES PAID
U.S. ENVIRONMENTAL PROTECTION AGENCY

EPA 335



*If your address is incorrect, please change on the above label
tear off, and return to the above address.
If you do not desire to continue receiving these technical
reports, CHECK HERE ☐, tear off label, and return it to the
above address.*